

宗务隆构造带西段三叠系隆务河组碎屑锆石特征 及其构造意义

赵文涛^{1,2}, 刘少峰¹, 陈 敏², 薛春纪^{1,2}

(1. 中国地质大学(北京) 地球科学与资源学院, 北京 100083; 2. 青海大学 地质工程系, 青海 西宁 810016)

摘要: 宗务隆构造带位于柴北缘构造带与南祁连构造带之间, 总体呈北西西向展布。构造带东段丰富的岩浆活动记录了该构造带晚古生代—中生代期间的裂解和闭合过程, 而西段岩浆活动的记录较为稀少, 对于其东、西段是否具有相同的构造演化尚不清晰。通过分析构造带西段三叠系隆务河组碎屑岩的地球化学特征、碎屑锆石 U-Pb 年龄及 Hf 同位素组成, 认为隆务河组的碎屑沉积物的源区古风化程度轻微, 不具备沉积再循环的特征, 原岩主要为长英质岩石, 南祁连新元古代花岗质片麻岩和早古生代大陆弧型花岗岩为隆务河组碎屑岩的主要物源; 碎屑岩可能沉积于早中三叠世挠曲型盆地中; 锆石 U-Pb 年龄分析表明宗务隆构造带东西段构造演化具有不同的历程, 东段发育有限洋盆, 而西段并未出现, 转换地带可能位于生格至罗根郭勒之间。

关键词: 宗务隆构造带; 隆务河组; 碎屑锆石; Hf 同位素

中图分类号: P578.94⁺¹; P597; P595

文献标识码: A

文章编号: 1000-6524(2022)03-0569-23

Detrital zircon characteristics of the Triassic Longwuhe Formation in the western segment of the Zongwulong tectonic belt and its tectonic significance

ZHAO Wen-tao^{1,2}, LIU Shao-feng¹, CHEN Min² and XUE Chun-ji^{1,2}

(1. School of Earth Sciences and Resources, China University of Geosciences(Beijing), Beijing 100083, China;

2. Geological Engineering Department, Qinghai University, Xining 810016, China)

Abstract: The Zongwulong tectonic belt is located between the northern Qaidam tectonic belt and the South Qilian tectonic belt, which is generally distributed in a NWW direction. The voluminous magmatic activity in the eastern part of the tectonic belt records the process of breakup and closure of the tectonic belt during the late Paleozoic Mesozoic, while the magmatic activity in the western part is relatively rare, so it is unclear whether the eastern and western parts of the belt have the same tectonic evolution. Based on the analysis of geochemical characteristics, detrital zircon U-Pb ages and Hf isotopic compositions of the clastic rocks of the Triassic Longwuhe Formation in the western part of the tectonic belt, it is considered that the provenance of the detrital sediments in the Longwuhe Formation was slightly weathered without sedimentary recycling characteristics, and their original rocks are mainly felsic rocks. The main provenance of clastic rocks in the Longwuhe Formation is the southern Qilian Neoproterozoic granitic gneiss and early Paleozoic continental arc granite rocks, and the clastic rocks may have been deposited in Early-Middle Triassic flexural basins. Zircon U-Pb age analysis shows that the tectonic evolution of the eastern and western

收稿日期: 2021-04-25; 接受日期: 2022-03-14; 编辑: 郝艳丽

基金项目: 2019 年度青海大学两级财政建设专项(41250103); 青海省自然科学基金项目(2019-ZJ-964); 青海省地质调查局项目(2018-SF-109)

作者简介: 赵文涛(1982-), 男, 博士研究生, 主要从事构造地质学方面的研究工作, E-mail: zhaowen168@163.com; 通讯作者: 刘少峰, 男, 博士生导师, 主要从事大陆动力学、沉积盆地构造分析和沉积学等方面的研究工作, E-mail: shaofeng@cugb.edu.cn。

segments of Zongwulong tectonic belt has different processes. Limited ocean basins developed in the eastern segment but not in the western segment, the transition zone may be located between Shengge and Luogenguole area.

Key words: Zongwulong tectonic belt; Longwuhe Formation; detrital zircon; Hf isotope

Fund support: Two-level financial construction project of Qinghai University (41250103); Natural science foundation of Qinghai Province (2019-ZJ-964); Strategic emerging mineral resources prospecting breakthrough and exploration technology demonstration project in the northern margin of Qaidam Basin (2018-SF-109).

土尔根大坂-宗务隆-青海南山构造带(简称宗务隆构造带)位于青海柴达木盆地以北区域,总体呈

北西西向展布,东部偏南东,西部偏北西,呈横卧“S”型(李平安等,1982)(图1)。宗务隆构造带

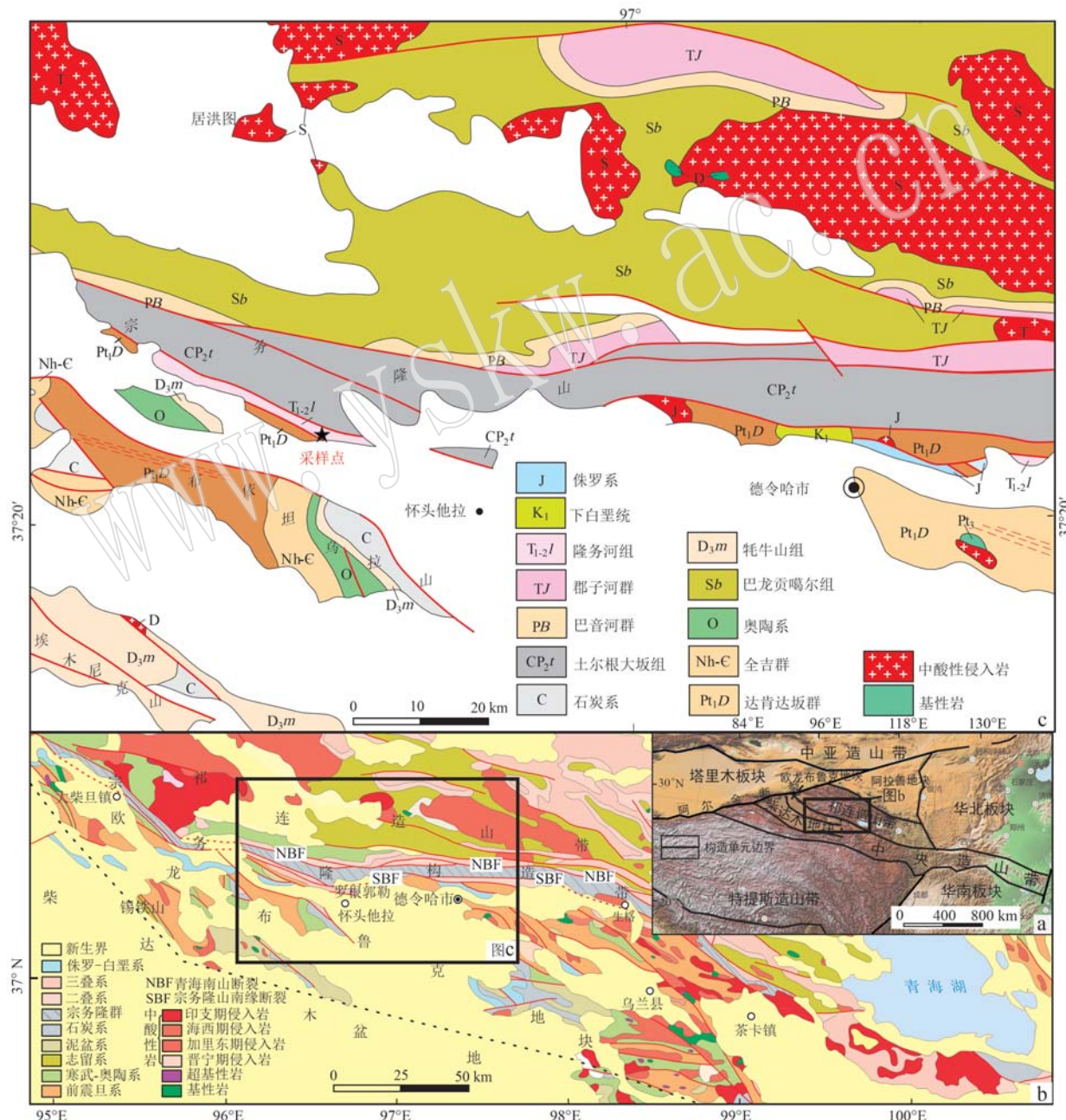


图 1 研究区地质简图 [a 据杨经绥等(2010)修改]

Fig. 1 Geological schematic map of the research area (modified from Yang Jingsui et al., 2010)

北以青海南山断裂(NBF)为界与南祁连造山带相邻, 南以宗务隆山南缘断裂(SBF)为界与柴北缘欧龙布鲁克地块相邻, 向西延至阿尔金断裂, 向东可能分割了西秦岭与南祁连造山带(图1b)(郭安林等, 2009)。众多学者根据宗务隆构造带内的沉积记录及其东段的岩浆活动, 认为宗务隆构造带晚古生代—中生代经历了由陆内裂陷、洋盆发育和从俯冲到碰撞造山的复杂演化过程(王毅智等, 2001; 孙延贵等, 2004; 彭渊, 2015; 王苏里等, 2016; 陈敏等, 2020)。但宗务隆构造带晚古生代—中生代的岩浆活动主要发育在其东段的乌兰一天峻南山一带, 对其构造-岩浆演化历史的研究也多聚焦于这一地区(郭安林等, 2009; 王苏里等, 2016; 彭渊等, 2016; Wu et al., 2019), 德令哈以西的西段则相对缺乏可以类比的岩浆记录, 因而, 其演化是否与东段相同并不清晰, 这直接制约了对整个宗务隆构造带形成和演化的全面认识。而宗务隆构造带夹持于中祁连地块、欧龙布鲁克地块和西秦岭之间, 对于理解祁连造山带、柴北缘造山带和西秦岭造山带构造演化及其构造衔接关系具有重要意义。

与造山带相关的盆地中, 沉积物可较完整且有代表性地保存造山带隆升和剥蚀过程信息, 对探讨造山带的构造演化具有至关重要的意义(McLennan et al., 2000; Roser et al., 2002; Joo et al., 2005)。沉积岩的碎屑成分能够有效地追索其主要的沉积物源, 探究物源区物质组成、构造环境及早期地壳的生长演化(McLennan et al., 1995)。锆石对物理-化学风化作用具有极强的抵抗力, 常可用于物源追索研究。地球化学和锆石年代学研究已经被广泛地应用于追踪物源区特征, 揭示碎屑沉积岩成因、古风化条件(Nesbitt and Young, 1982; McLennan et al., 1995; Roser et al., 2002)和恢复沉积盆地构造环境(Bhatia, 1983; Roser and Korsch, 1988; Fedo et al., 1995)。

宗务隆构造带西段早中三叠世隆务河组的沉积过程应当记录了该地区前中生代的构造-热事件。本文利用岩石地球化学、LA-ICP-MS法U-Pb定年以及Lu-Hf同位素分析技术, 研究发育在宗务隆构造带西段的隆务河组碎屑岩, 分析其物源和沉积构造环境, 并限定其沉积年代, 利用锆石的年龄谱信息追溯其物源区的构造-热事件, 以期对宗务隆构造带西段的构造演化和地球动力学过程提供更多的证据。

1 地质背景

宗务隆构造带北与南祁连造山带相邻, 南与欧龙布鲁克地块、柴北缘结合带滩间山岩浆弧相邻(张雪亭等, 2010; 付长磊等, 2021)。区内地层出露较全, 自古元古代至新生代的地层均有不同程度的发育, 主要的地层有:

古元古界达肯大坂岩群为区内最古老的地层, 是欧龙布鲁克地块的结晶基底。地层由于历遭多期断裂构造的切割破坏、岩浆的侵蚀及后期沉积岩系的掩盖, 多呈不连续的块体分布于宗务隆构造带的南侧。年代学研究显示其具有 $2.5\sim2.3\text{ Ga}$ 的形成年龄和 $1.9\sim1.8\text{ Ga}$ 的变质年龄(Song et al., 2006; Lu et al., 2008; Chen et al., 2009; Liao et al., 2014; Wang et al., 2016; 路增龙等, 2017; Yu et al., 2017; Wang et al., 2019; 张建新等, 2021)。

全吉群是欧龙布鲁克地块中覆盖于达肯达坂群之上的一套盖层沉积。对于其时代归属, 早期的区调工作将其划为南华系一下寒武统的连续沉积, 为多数学者及基础地质资料沿用, 但张海军等(2016)在其中识别出一个平行不整合面, 并结合其中得到的凝灰岩U-Pb年龄($1\ 640\pm15\text{ Ma}$ 和 $1\ 646\pm20\text{ Ma}$), 将其时代限定为长城系—震旦系。

巴龙贡嘎尔组为一套轻微变质岩系, 主要分布在宗务隆构造带北侧的南祁连地区, 总体构造线方向为NWW向, 由灰、浅灰绿色厚层片状砂岩、深灰绿色厚层硬砂岩夹板岩、凝灰岩、硅质岩组成。前期将其划为志留系(张雪亭等, 2010), 但近年来, 对本地层的年代学研究取得了一系列新的认识, 有学者在其中识别出新元古代地层, 从中解体出拐杖山组(计波等, 2018, 2021)。通过地层中的火山岩夹层的年代学研究, 牛广智等(2016)于该套地层中的英安质火山熔岩获得了 $457.6\pm2.4\text{ Ma}$ 的U-Pb年龄(LA-ICP-MS), 表明该套火山岩形成于晚奥陶世; 李大磊等(2018)在该套地层中的变玄武安山岩获得了 $427.2\pm2.8\text{ Ma}$ 的锆石U-Pb年龄(LA-ICP-MS), 认为该套火山岩形成于早志留世; 潘建等(2019)在该地层中的基性火山岩中获取锆石U-Pb年龄为 $819\pm2\text{ Ma}$, 表明其形成时代为新元古代; 贺小元等(2021)在该地层中获得英安岩-流纹岩的锆石U-Pb年龄为 $438.1\pm2.2\sim403.0\pm2.6\text{ Ma}$, 说明火山岩形成于早志留世—早泥盆世。也有学者通过碎屑锆石

研究,认为其沉积时代在新元古代至早古生代(秦宇,2018; Li et al., 2019; Yan et al., 2020)。总体看来,巴龙贡噶尔组应当是一套新元古代—早古生代的沉积物,是原特提斯洋演化过程的产物。

下古生界主要分布于欧龙布鲁克中、东段及石灰沟等一带地区,中上寒武统欧龙布鲁克群($\epsilon_{2,3}$ O)为一套碳酸盐岩沉积,下部夹有少量碎屑岩(孙娇鹏等,2015),奥陶系仅发育下奥陶统多泉山组和石灰沟组,主要为浅海相碳酸盐-笔石页岩沉积建造(马帅等,2016)。晚古生代发育有上泥盆统的牦牛山组陆相磨拉石、下石炭统城墙沟组和怀头他拉组稳定被动陆缘沉积(孙娇鹏等,2016)及石炭-二叠系的宗务隆群。宗务隆群是宗务隆构造带内最主要的沉积记录,广泛分布于构造带内,下部的土

尔根大坂组主要为碎屑岩夹火山岩建造,上部果可山组主要为浅海相岩屑石英砂岩夹灰岩组合(李平安等,1982; 孙娇鹏等,2015, 付长奎等,2021)。

早中三叠世隆务河组($T_{1-2}l$)在构造带的西段主要呈条状分布于宗务隆构造带怀头他拉附近,总体岩性特征为一套灰绿色-灰黑色-黑灰色砂岩、板岩夹薄层灰岩,局部地段往上开始出现砾岩夹砂岩,砾石成分复杂多变,总体呈现出向上变粗的趋势,磨圆往上亦逐渐变好(刘奎等,2020),从砾石成分复杂、砾径大小悬殊、磨圆度不均一来看,为山麓洪积相堆积,具有磨拉石建造的特征。与西段不同,在构造带的东段,隆务河组分布广泛,自橡皮山地区向东,与西秦岭造山带的隆务河组可以对比(图2),为典型的复理石碎屑岩沉积(彭志军等,2016)。

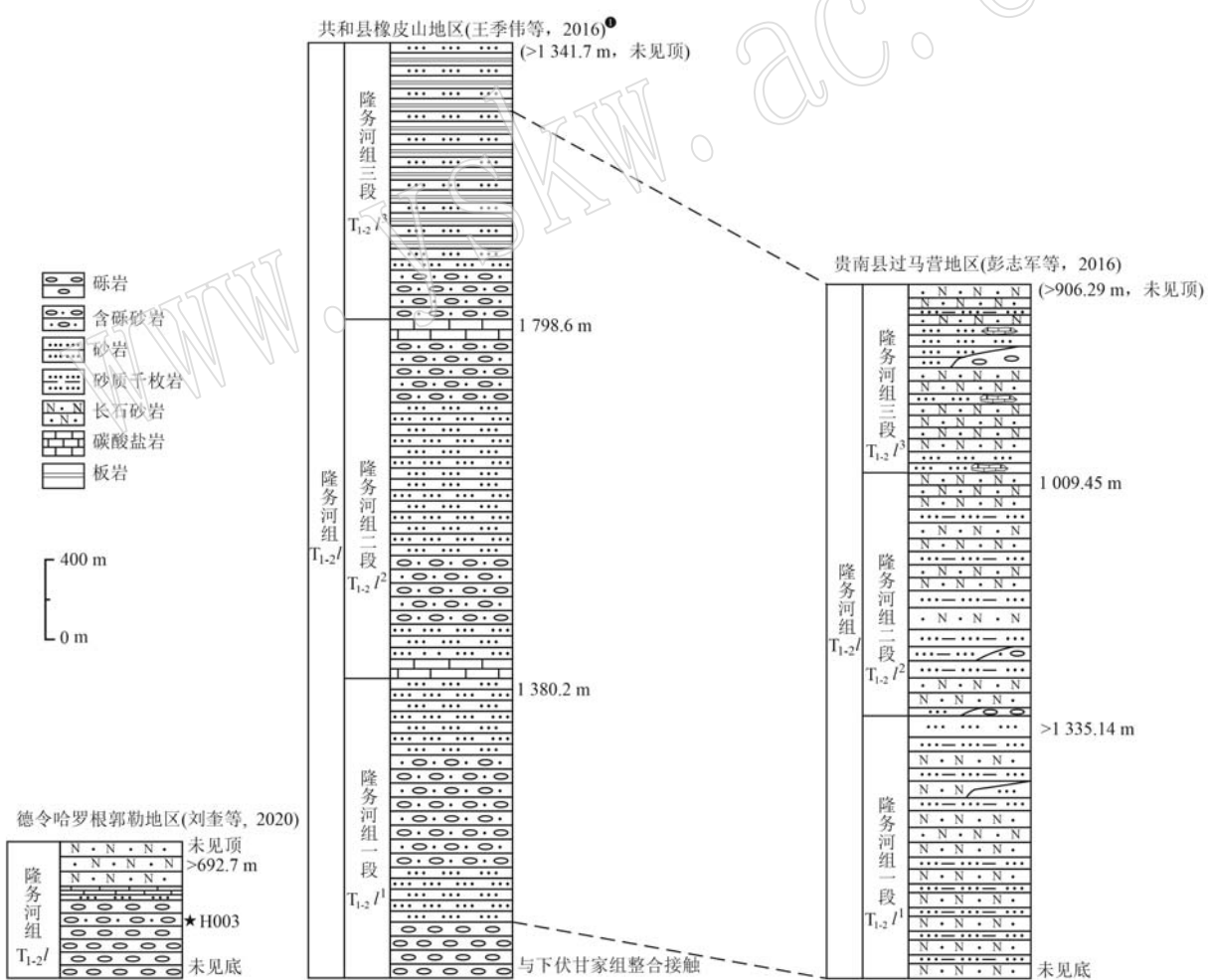


图2 隆务河组区域地层柱状对比图

Fig. 2 Regional stratigraphic columnar correlation map of Longwuhe Formation

① 王季伟,赵瑞强,赵志成,等. 2016. 大水桥幅(J47E020014)1:5万区域地质图.

宗务隆构造带大致经历了泥盆-石炭纪的裂解(孙延贵等, 2004; 彭渊, 2015)、二叠纪-中三叠世的俯冲和晚三叠世的碰撞作用(王毅智等, 2001; 郭安林等, 2009; 王苏里等, 2016; 彭渊等, 2016; Wu et al., 2019), 并且之后还受到青藏高原隆升的影响, 因而其构造十分复杂, 褶皱构造和断裂构造极为发育。除中更新世以后地层未经受过褶皱构造变动外, 其余各时代地层均遭受过不同程度的褶皱变动。发育有宗务隆山-青海南山北缘主边界断裂(NBF)和宗务隆山南缘断裂(SBF)两条主要断裂(图1b), 这两条边界断裂控制了宗务隆裂谷的形成与演化, 并在后期裂谷闭合的过程中发生了反转, 现均表现为以逆冲推覆为主要特征的区域性断裂(张雪亭等, 2010; 彭渊, 2015)。

研究区的岩浆活动以新元古代—早古生代和晚古生代最为强烈, 前者主要反映了柴北缘和南祁连的加里东期的造山事件, 后者则集中在构造带的东段, 反映了晚古生代—中生代的构造事件。

2 样品特征与测试方法

2.1 样品特征

样品H003采自宗务隆构造带德令哈罗根郭勒地区下中三叠统隆务河组中, 采样位置为E96°44'

09.36", N37°24'48.89"(图2)。

样品野外露头如图3a所示。样品为灰色含砾不等粒岩屑长石砂岩, 具含砾不等粒砂状结构, 块状构造(图3b)。岩石由碎屑(约82%)、杂基(约10%)和胶结物(约8%)组成(图3c)。碎屑成分主要由石英(55%)、长石(25%)(斜长石>钾长石)、岩屑(15%)(石英岩、板岩、火山岩等)、黑云母(2%)、白云母(少量)、铁铝榴石(1%)、绿帘石(1%)、不透明金属矿物(1%)等组成。杂基主要由绿泥石(7%)和绢云母(1%)等组成。胶结物为显微粒状石英。碎屑分选性较差, 粒径大小绝大多数在0.06~2.0 mm之间, 少数达到细砾级, 粒径在2.0~3.52 mm之间。碎屑磨圆度相对较好, 多数呈次棱角状, 少数呈棱角状, 个别呈次圆状, 球度一般, 粗、中、细不同粒级的碎屑共存且含量大致相当, 呈不等粒状分布。杂基成分为粘土矿物重结晶的绿泥石、绢云母, 呈细小鳞片状结合体, 在岩石中不均匀分布于碎屑颗粒接触处。胶结物成分为显微粒状石英, 在岩石中不均匀充填于碎屑颗粒间隙。胶结类型为孔隙式胶结。

2.2 测试方法

样品的主微量元素分析由河北省区域地质矿产调查研究所实验室完成。样品首先无污染粉碎至200目, 主量元素测试分析采用 Axios max X射线

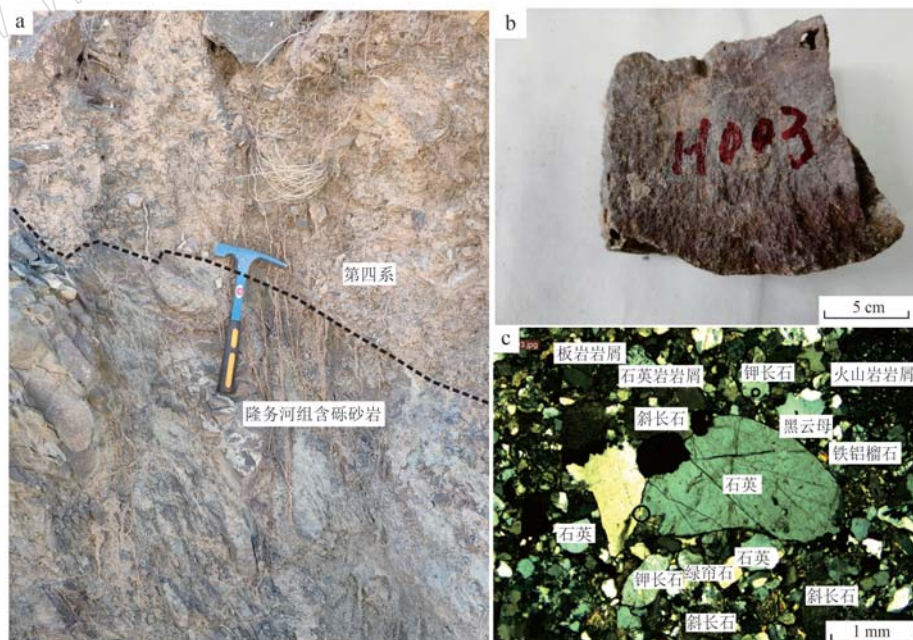


图3 隆务河组砂岩样品的基本特征

Fig. 3 Basic characteristics of the samples

a—野外露头; b—手标本; c—显微照片(正交偏光)

a—outcrop; b—hand specimen; c—microphotograph(crossed nicols)

荧光光谱仪完成, 稀土微量元素分析采用 X Series2 电感耦合等离子体质谱仪完成。锆石 U-Pb 定年样品经人工破碎后按照常规方法分选锆石, 在双目镜下挑选透明、晶形完好的锆石颗粒, 粘于环氧树脂表面, 固化后抛光至露出一个光洁平面, 然后进行透、反射光和阴极发光(CL)照相, 结合这些图像选择最佳锆石进行定年测试。测试分析在南京宏创地质勘查技术服务有限公司微区分析实验室使用激光剥蚀-电感耦合等离子体质谱仪(LA-ICPMS)完成。激光剥蚀平台采用 Resolution SE 型 193 nm 深紫外激光剥蚀进样系统, 配备 S155 型双体积样品池。质谱仪采用 Agilent 7900 型电感耦合等离子体质谱仪, 具体测试方法参见 Liu 等(2010)。Hf 同位素测试使用 193 nm ArF 准分子激光剥蚀系统, 由 Australian Scientific Instruments 制造, 型号为 RESolution LR。多接收器型号电感耦合等离子体质谱仪(MC-ICP-MS)由英国 Nu Instruments 公司制造, 型号为 Nu Plasma II。准分子激光发生器产生的深紫外光束经匀化光路聚焦于锆石表面, 能量密度为 3.5 J/cm², 束斑直径为 50 μm, 频率为 8 Hz, 共剥蚀 40 s, 剥蚀气溶胶由氦气送入 MC-ICP-MS 完成测试。测试过程中每测 5 颗样品锆石, 依次测试 1 颗标准锆石(包括 GJ-1、91500、Plešovice Mud Tank、Penglai), 以检验锆石 Hf 同位素比值数据质量。

3 测试结果

3.1 全岩地球化学测试结果

3.1.1 主量元素特征

样品的主量元素测试结果(表 1)显示, 样品中 SiO₂ 的含量较高, 含量变化范围较小, 为 69.69%~74.46%, 平均为 73.11%, 略高于 UCC(大陆上地壳)及 PAAS(北美页岩)。Al₂O₃ 的含量在 10.52%~12.83%, 平均为 11.13%, 低于 UCC 及 PAAS; 岩石全碱 K₂O+Na₂O 为 4.60%~5.28%, 平均为 4.82%, 与 PAAS 相近, 低于 UCC, 显示全碱含量较低; MnO、MgO、P₂O₅ 和 CaO 的含量也较低。

3.1.2 微量元素与稀土元素特征

样品微量元素含量和特征参数(表 1)经过 UCC 标准化后, 过渡族元素(Sc、V、Cr、Cu、Co、Ni)显示不同程度的亏损(图 4a)。过渡族元素在沉积-成岩过程中可有效保持源岩的地球化学特征, 因而强烈

表 1 样品的主量元素($w_B/\%$)和微量元素($w_B/10^{-6}$)分析结果

Table 1 Analysis results of major ($w_B/\%$) and trace ($w_B/10^{-6}$) elements

样品编号	H003-1	H003-2	H003-3	H003-4	PAAS	UCC
SiO ₂	73.90	74.46	69.69	74.37	62.80	66.60
Al ₂ O ₃	10.60	10.52	12.83	10.57	18.90	15.40
TiO ₂	0.48	0.48	0.60	0.49	1.00	0.64
Fe ₂ O ₃ ^T	4.36	4.05	4.60	4.41	6.50	5.04
CaO	1.15	1.43	1.93	1.37	1.30	3.59
MgO	2.06	1.82	2.15	1.83	2.20	2.48
K ₂ O	2.82	2.79	2.35	2.87	3.70	2.80
Na ₂ O	1.85	1.95	2.93	1.73	1.20	3.27
MnO	0.065	0.064	0.069	0.070	0.10	0.10
P ₂ O ₅	0.117	0.108	0.160	0.123	0.16	0.15
ICV	1.56	1.55	1.53	1.53	0.88	1.70
CIA	57.21	55.08	54.98	56.45	70	48
PIA	59.42	56.31	55.22	58.30	82	57
Y	20.19	21.84	23.39	23.29	27.00	21.00
La	27.97	34.88	48.72	33.45	38.20	31.00
Ce	48.97	61.47	85.07	61.86	79.60	63.00
Pr	6.46	7.60	10.35	7.53	8.83	7.10
Nd	23.37	26.73	36.36	26.10	33.90	27.00
Sm	4.26	4.69	6.12	5.13	5.55	4.70
Eu	2.00	1.83	2.09	0.61	1.08	1.00
Gd	3.82	4.37	5.53	5.08	4.66	4.00
Tb	0.63	0.67	0.79	0.70	0.77	0.70
Dy	3.84	4.01	4.52	4.19	4.68	3.90
Ho	0.76	0.78	0.85	0.87	0.99	0.83
Er	2.17	2.26	2.46	2.60	2.85	2.30
Tm	0.36	0.37	0.39	0.39	0.41	0.30
Yb	2.28	2.32	2.47	2.53	2.82	2.00
Lu	0.36	0.36	0.39	0.38	0.44	0.31
Sc	9.45	10.19	12.19	9.01	16.00	14.00
V	62.36	68.12	65.54	59.53	150.00	97.00
Cr	40.29	44.20	46.46	93.90	110.00	92.00
Co	10.00	9.72	10.66	8.30	23.00	17.30
Ni	21.37	20.50	19.47	19.47	55.00	47.00
Cu	7.43	9.21	8.34	4.97	50.00	28.00
Zn	50.07	45.42	46.64	51.28	85.00	67.00
Rb	91.34	97.84	70.46	81.40	160.00	82.00
Sr	270.44	300.93	349.23	329.20	200.00	320.00
Zr	138.06	159.24	197.41	190.80	210.00	193.00
Ba	3 380.13	2 819.69	2 878.45	5 033.00	650.00	628.00
Hf	4.04	4.26	5.48	5.21	5.00	5.30
Pb	18.83	23.63	19.89	22.41	20.00	17.00
Th	11.87	13.42	14.09	12.90	14.60	10.50
U	1.65	1.74	1.84	2.15	3.10	2.70
ΣREE	127.25	152.34	206.11	151.42	184.78	148.14
LREE	113.04	137.2	188.71	134.69	167.16	133.8
HREE	14.20	15.13	17.41	16.74	17.62	14.34
LREE/HREE	7.96	9.07	10.84	8.05	9.49	9.33
La _N /Yb _N	8.82	10.79	14.15	9.47	9.72	11.12
δEu	1.52	1.24	1.10	0.37	0.65	0.71
δCe	0.89	0.93	0.93	0.96	1.06	1.04

CIA=[Al₂O₃/(Al₂O₃+CaO^{*}+Na₂O+K₂O)]×100(摩尔数)(Nesbitt and Young, 1982), CaO^{*}仅指硅酸盐矿物中的 CaO, 采用 McLennan(1993)的方法计算(CaO^{**}=CaO-10/3×P₂O₅, 其中如果 CaO^{**}<Na₂O, 则 CaO^{*}=CaO^{**}, 否则 CaO^{*}=Na₂O(Fedo et al., 1995)); ICV=(Fe₂O₃+K₂O+Na₂O+CaO+MgO+MnO+TiO₂)/Al₂O₃(摩尔比)(Cox et al., 1995); PIA=[(Al₂O₃-K₂O)/(Al₂O₃+CaO+Na₂O-K₂O)]×100(摩尔数)(Fedo et al., 1995); PAAS 据 Taylor and McLennan(1985); UCC 据 Rudnick and Gao(2003)。

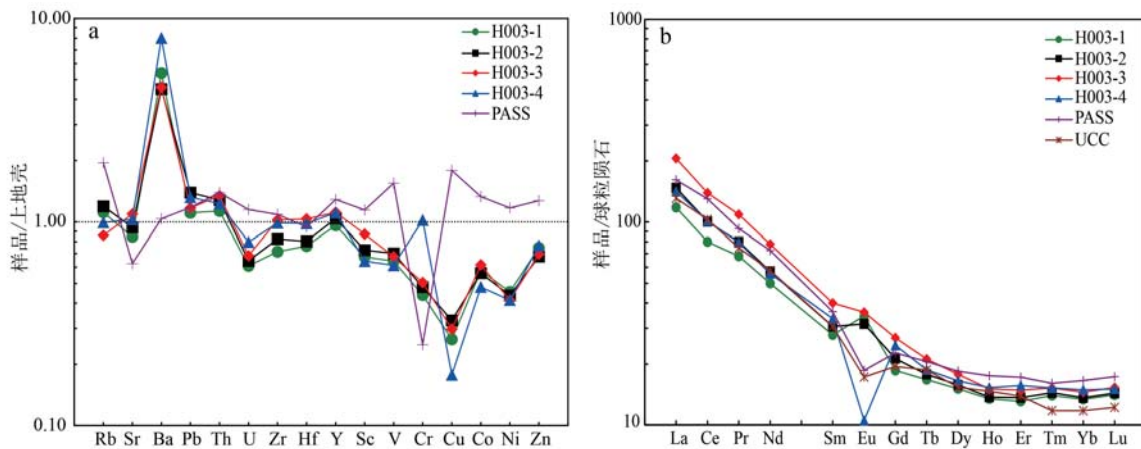


图4 隆务河组碎屑岩大陆上地壳标准化微量元素蛛网图(a)和球粒陨石标准化稀土元素配分曲线(b)
Fig. 4 Upper continental crust-normalized trace elements spider diagram (a) and chondrite-normalized REE patterns (b) of the
Longwuhe Formmation clastic rocks
UCC 据 Rudnick and Gao(2003); 球粒陨石据 Sun and McDonough(1989); PAAS 据 Taylor and McLennan(1985)
UCC from Rudnick and Gao, 2003; Chondrite from Sun and McDonough, 1989; PAAS from Taylor and McLennan, 1985

富集过渡族元素为特征的基性-超基性岩应当不是样品的主要源岩。大离子亲石元素(LILE)Rb、Th表现出弱富集, U 表现为弱亏损的特征。Ba 强烈富集, 高场强元素 Hf、Y、Zr 相对于 UCC 表现出弱亏损的特征。Sr 含量变化范围不大, 与 UCC 含量相近。

样品稀土元素含量和特征参数见表 1, 球粒陨石标准化的稀土元素配分模式如图 4b 所示。 Σ REE 为 $127.23 \times 10^{-6} \sim 206.12 \times 10^{-6}$, 平均 159.28×10^{-6} , 与 UCC 相近, 低于 PAAS, 反映出样品相对富集稀土元素的特征。样品 LREE / HREE 为 7.96 ~ 10.84, 均值为 8.98, 略低于 PAAS 和 UCC 的比值, (La/Yb)_N 值为 8.82 ~ 14.15, 平均值为 10.81, 低于 UCC, 高于 PAAS, 表明轻重稀土元素分馏程度中

等。样品的 Eu 除 H003-4 外均显示正异常, 除受斜长石风化程度的影响外, 可能与样品中 Ba 元素的强烈富集有关。

3.2 碎屑锆石 U-Pb 年龄的测试结果

锆石是一种稳定的重矿物, 其成分和年龄不受沉积过程的影响, 是判别物源特征最有效的证据之一(Cawood and Nemchin, 2000; Hallsworth *et al.*, 2000)。本次工作的样品所取得的年龄数据详见表 2。

样品的碎屑锆石大多为自形或半自形晶, 晶体多呈粒状或椭球状, 少量为短柱状、锥状。锆石粒径一般在 50 ~ 150 μm 之间, 长宽比在 1:1 ~ 2:1 之间。CL 图像显示(图 5), 锆石的发光性总体较低,

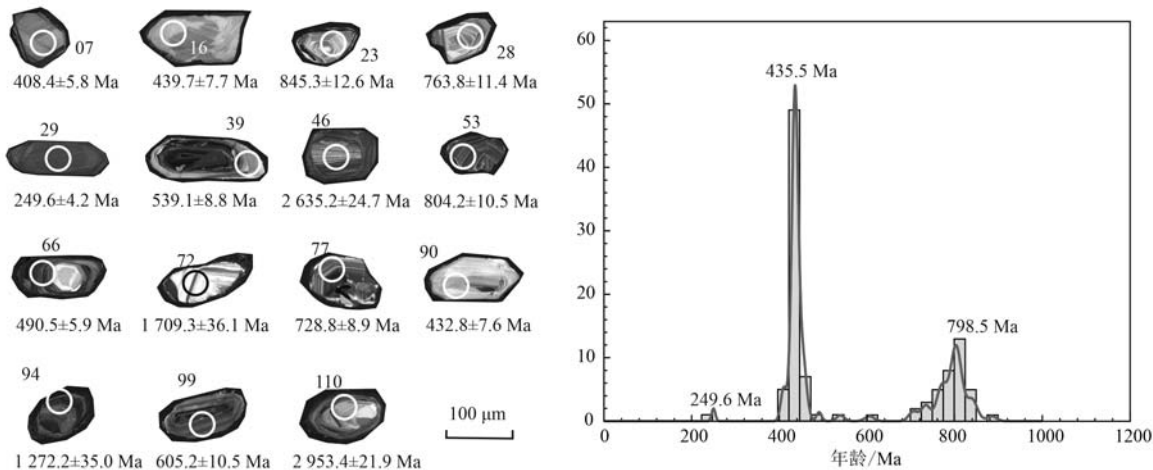


图5 隆务河组代表性碎屑锆石 CL 图像及年龄分布直方图
Fig. 5 CL images and age distribution histogram of representative detrital zircons from the Longwuhe Formation

表 2 隆务河组碎屑岩锆石 U-Pb 年龄分析结果
Table 2 LA-ICP-MS zircon U-Pb dating results for the Longwuhe Formation clastic rocks

测点	$w_{\text{B}}/10^{-6}$		Th/U	同位素比值						年龄/Ma			谐和度			
	^{232}Th	^{238}U		$^{207}\text{Pb}/^{206}\text{Pb}$	1σ	$^{207}\text{Pb}/^{235}\text{U}$	1σ	$^{206}\text{Pb}/^{238}\text{U}$	1σ	$^{207}\text{Pb}/^{206}\text{Pb}$	1σ	$^{207}\text{Pb}/^{235}\text{U}$	1σ			
1	167.71	276.39	0.61	0.163 4	0.002 5	10.261 5	0.190 7	0.453 3	0.006 7	2.491.7	25.6	2.458.6	17.3	2.409.9	29.8	97%
2	160.75	314.16	0.51	0.054 6	0.001 5	0.529 7	0.014 6	0.070 4	0.001 0	394.5	61.1	431.6	9.7	438.5	6.0	98%
3	53.98	95.15	0.56	0.056 4	0.002 1	0.535 7	0.020 4	0.069 3	0.001 1	464.9	78.7	435.6	13.5	431.9	6.8	99%
4	54.75	104.03	0.53	0.056 5	0.002 2	0.540 3	0.020 6	0.069 5	0.001 2	472.3	83.3	438.6	13.6	433.4	7.1	98%
5	100.34	219.21	0.46	0.057 4	0.001 5	0.558 3	0.015 3	0.070 4	0.001 0	505.6	55.6	450.4	10.0	438.3	5.8	97%
6	144.71	316.61	0.46	0.057 0	0.001 5	0.554 5	0.014 7	0.070 4	0.001 1	500.0	55.6	447.9	9.6	438.7	6.3	97%
7	73.30	175.63	0.42	0.056 1	0.001 9	0.506 7	0.015 5	0.065 4	0.001 0	457.5	74.1	416.2	10.4	408.4	5.8	98%
8	216.03	379.90	0.57	0.066 9	0.001 2	1.247 9	0.026 6	0.134 6	0.001 9	833.0	40.9	822.4	12.0	814.2	11.0	98%
9	117.39	823.89	0.14	0.055 4	0.001 1	0.562 6	0.012 1	0.073 5	0.001 0	427.8	44.4	453.2	7.8	456.9	5.8	99%
10	318.06	187.97	1.69	0.066 0	0.001 4	1.196 4	0.026 1	0.131 6	0.001 7	805.6	44.4	798.9	12.1	796.8	10.0	99%
11	440.07	849.37	0.52	0.064 8	0.001 1	1.085 2	0.019 6	0.121 1	0.001 5	768.5	36.3	746.2	9.5	736.7	8.5	98%
12	141.41	276.53	0.51	0.053 8	0.001 3	0.521 3	0.014 4	0.069 9	0.000 9	364.9	53.7	426.0	9.6	435.6	5.7	97%
13	500.07	469.80	1.06	0.065 1	0.001 7	0.588 4	0.014 7	0.065 8	0.000 9	788.9	55.6	469.8	9.4	410.6	5.5	86%
14	285.32	226.97	1.26	0.065 6	0.001 7	1.208 9	0.029 8	0.133 5	0.002 3	792.3	55.6	804.7	13.7	807.6	12.9	99%
15	154.46	292.28	0.53	0.067 2	0.001 3	1.189 2	0.025 9	0.127 9	0.001 8	844.1	-158.3	795.6	12.0	776	10.3	97%
16	50.84	91.49	0.56	0.055 9	0.002 5	0.535 7	0.023 0	0.070 6	0.001 3	455.6	101.8	435.6	15.2	439.7	7.7	99%
17	112.39	240.07	0.47	0.065 7	0.001 3	1.215 6	0.028 3	0.133 7	0.002 0	798.2	42.6	807.8	13.0	808.8	11.7	99%
18	102.20	136.32	0.75	0.165 2	0.002 6	10.422 8	0.188 5	0.456 1	0.006 7	2.510.2	26.2	2.473.1	16.8	2.422.3	29.7	97%
19	196.62	146.23	1.34	0.064 6	0.001 7	1.142 5	0.032 6	0.128 1	0.001 8	761.1	57.4	773.7	15.5	777.2	10.5	99%
20	136.28	348.28	0.39	0.055 3	0.001 4	0.555 4	0.015 3	0.072 8	0.001 1	433.4	59.3	448.5	10.0	453.3	6.6	98%
21	74.81	118.44	0.63	0.067 0	0.002 2	1.221 8	0.045 6	0.131 1	0.002 5	838.9	68.5	810.6	20.9	794.3	14.5	97%
22	63.76	106.00	0.60	0.054 9	0.002 4	0.528 0	0.025 0	0.069 2	0.001 3	405.6	98.1	430.5	16.6	431.5	8.1	99%
23	100.92	122.94	0.82	0.065 4	0.001 7	1.267 0	0.037 2	0.140 1	0.002 2	787.0	55.6	831.1	16.7	845.3	12.6	98%
24	142.68	213.20	0.67	0.057 3	0.001 5	0.574 0	0.015 5	0.072 7	0.001 2	501.9	55.6	460.6	10.0	452.2	7.0	98%
25	151.27	308.58	0.49	0.054 9	0.001 8	0.531 7	0.019 2	0.069 7	0.001 2	405.6	74.1	432.9	12.8	434.3	7.3	99%
26	213.83	636.22	0.34	0.055 4	0.001 2	0.539 6	0.012 9	0.070 2	0.001 1	427.8	43.5	438.2	8.5	437.3	6.8	99%
27	48.66	71.96	0.68	0.054 6	0.002 4	0.512 9	0.021 5	0.068 5	0.001 4	398.2	100.9	420.4	14.4	427.4	8.3	98%
28	140.12	117.77	1.19	0.066 6	0.001 9	1.161 2	0.034 2	0.125 8	0.002 0	827.8	59.7	782.5	16.1	763.8	11.4	97%
29	10.07	295.06	0.03	0.051 2	0.001 8	0.280 5	0.010 1	0.039 5	0.000 7	255.6	77.8	251.0	8.0	249.6	4.2	99%
30	122.45	263.91	0.46	0.055 3	0.001 7	0.539 0	0.017 3	0.069 8	0.001 1	433.4	73.1	437.7	11.4	435.0	6.7	99%
31	186.15	252.57	0.74	0.055 4	0.001 9	0.538 4	0.019 6	0.069 6	0.001 3	431.5	75.9	437.4	12.9	433.9	7.7	99%
32	87.99	178.88	0.49	0.056 6	0.002 2	0.514 5	0.019 0	0.065 4	0.001 2	476.0	88.0	421.5	12.7	408.4	7.3	96%
33	165.89	646.79	0.26	0.056 9	0.001 6	0.589 5	0.016 3	0.074 3	0.001 3	487.1	59.3	470.6	10.4	462.0	7.7	98%
34	88.43	296.62	0.30	0.055 2	0.001 6	0.550 9	0.015 9	0.071 7	0.001 2	420.4	64.8	445.6	10.4	446.5	7.0	99%
35	48.23	172.36	0.28	0.055 2	0.001 9	0.567 6	0.021 9	0.073 6	0.001 5	420.4	77.8	456.4	14.2	458.1	9.3	99%
36	90.45	116.99	0.77	0.065 5	0.002 1	1.164 5	0.033 8	0.126 9	0.001 9	790.7	66.7	784.1	15.9	770.0	11.0	98%
37	236.32	366.78	0.64	0.065 7	0.001 7	1.048 2	0.025 9	0.114 9	0.001 6	798.2	53.7	728.0	12.8	701.1	9.3	96%

续表 2-1
Continued Table 2-1

测点	$w_{\text{B}}/10^{-6}$		同位素比值		年龄/Ma											
	^{232}Th	^{238}U	Th/U	$^{207}\text{Pb}/^{206}\text{Pb}$	1σ	$^{207}\text{Pb}/^{235}\text{U}$	1σ	$^{206}\text{Pb}/^{238}\text{U}$	1σ	$^{207}\text{Pb}/^{206}\text{Pb}$	1σ	$^{207}\text{Pb}/^{235}\text{U}$	1σ	$^{206}\text{Pb}/^{238}\text{U}$	1σ	谐和度
38	208.16	303.89	0.68	0.0559	0.0017	0.5081	0.0155	0.0653	0.0010	450.0	66.7	417.1	10.4	408.1	5.9	97%
39	70.75	455.04	0.16	0.0599	0.0013	0.7265	0.0184	0.0872	0.0015	598.2	52.8	554.5	10.8	539.1	8.8	97%
40	132.88	216.27	0.61	0.0664	0.0016	1.2132	0.0307	0.1320	0.0020	816.7	56.5	806.7	14.1	799.1	11.2	99%
41	74.64	140.16	0.53	0.0554	0.0020	0.5351	0.0202	0.0702	0.0012	427.8	83.3	435.2	13.4	437.2	7.5	99%
42	242.46	167.09	1.45	0.0533	0.0017	0.5100	0.0166	0.0695	0.0011	338.9	74.1	418.4	11.2	432.9	6.5	96%
43	151.55	390.5	0.39	0.0558	0.0013	0.5412	0.0151	0.0695	0.0010	455.6	51.8	439.2	9.9	433.3	6.0	98%
44	96.27	129.18	0.75	0.1713	0.0025	11.3297	0.1994	0.4762	0.0063	2.572.2	24.7	2.550.7	16.5	2.510.9	27.4	98%
45	172.68	202.46	0.85	0.0677	0.0017	1.2394	0.0312	0.1314	0.0018	858.9	50.0	818.6	14.2	796.0	10.1	97%
46	94.62	167.68	0.56	0.1779	0.0026	10.3862	0.1910	0.4206	0.0060	2.635.2	24.7	2.469.8	17.1	2.263.2	27.1	91%
47	205.38	299.12	0.69	0.0680	0.0013	1.3849	0.0294	0.1471	0.0019	877.8	41.8	882.5	12.5	884.5	10.8	99%
48	106.94	265.77	0.40	0.0552	0.0016	0.5353	0.0145	0.0697	0.0011	420.4	64.8	435.3	9.6	434.3	6.3	99%
49	96.09	266.56	0.36	0.0554	0.0018	0.5345	0.0156	0.0698	0.0011	431.5	67.6	434.8	10.3	435.0	6.7	99%
50	133.41	471.89	0.28	0.0672	0.0012	1.2241	0.0248	0.1318	0.0020	842.6	37.0	811.7	11.3	798.3	11.2	98%
51	124.78	186.9	0.67	0.0556	0.0018	0.5374	0.0167	0.0698	0.0011	438.9	72.2	436.7	11.1	435.3	6.5	99%
52	63.41	194.79	0.33	0.0557	0.0019	0.5388	0.0171	0.0701	0.0011	442.6	78.7	437.7	11.3	436.9	6.4	99%
53	251.63	395.97	0.64	0.0666	0.0012	1.2224	0.0255	0.1329	0.0018	827.8	38.9	810.9	11.7	804.2	10.5	99%
54	59.24	94.68	0.63	0.0576	0.0024	0.5429	0.0219	0.0696	0.0012	522.3	95.4	440.3	14.4	433.7	7.2	98%
55	67.00	153.05	0.44	0.0564	0.0018	0.5579	0.0194	0.0718	0.0014	477.8	100.9	450.2	12.6	447.3	8.3	99%
56	79.53	143.76	0.55	0.0555	0.0020	0.5356	0.0196	0.0696	0.0011	431.5	79.6	435.5	13.0	433.5	6.9	99%
57	266.82	258.5	1.03	0.0666	0.0013	1.1141	0.0257	0.1211	0.0018	825.6	47.2	760.1	12.3	737.1	10.4	96%
58	129.71	215.93	0.60	0.0561	0.0016	0.5406	0.0149	0.0703	0.0011	457.5	63.0	438.8	9.8	437.7	6.7	99%
59	41.82	81.58	0.51	0.0748	0.0032	0.6906	0.0310	0.0665	0.0010	1.064.8	87.0	533.2	18.6	415.3	6.1	75%
60	111.25	356.85	0.31	0.0563	0.0019	0.5449	0.0143	0.0701	0.0010	464.9	74.1	441.6	9.4	436.6	6.2	98%
61	215.80	155.34	1.39	0.0633	0.0016	1.1049	0.0305	0.1259	0.0019	720.4	53.7	755.7	14.7	764.3	10.7	98%
62	113.09	163.27	0.69	0.0704	0.0018	1.2502	0.0329	0.1282	0.0018	939.8	51.9	823.5	14.9	777.8	10.1	94%
63	137.17	255.72	0.54	0.0559	0.0015	0.5419	0.0148	0.0703	0.0012	450	57.4	439.7	9.7	437.8	6.9	99%
64	170.60	432.65	0.39	0.0558	0.0013	0.5352	0.0131	0.0693	0.0010	455.6	51.8	435.2	8.7	431.6	6.1	99%
65	98.11	175.96	0.56	0.0545	0.0017	0.5264	0.0175	0.0698	0.0012	390.8	70.4	429.4	11.6	435.0	7.5	98%
66	209.42	460.52	0.45	0.0588	0.0014	0.5462	0.0157	0.0791	0.0010	561.1	51.8	506.1	9.7	490.5	5.9	96%
67	191.17	226.48	0.84	0.0656	0.0014	1.2064	0.0292	0.1326	0.0021	794.4	46.3	803.6	13.5	802.5	11.8	99%
68	91.46	191.5	0.48	0.0554	0.0018	0.5343	0.0183	0.0696	0.0011	427.8	72.2	434.7	12.1	433.5	6.4	99%
69	148.63	363.4	0.41	0.1651	0.0026	10.5933	0.3123	0.4563	0.0109	2.509	27.2	2.488.1	27.4	2.423.3	48.3	95%
70	96.03	311.59	0.31	0.0556	0.0014	0.5337	0.0130	0.0693	0.0010	438.9	55.6	434.3	8.6	432.1	5.8	99%
71	76.95	350.83	0.22	0.0530	0.0014	0.5053	0.0145	0.0688	0.0011	331.5	28.7	415.3	9.8	428.9	6.5	96%
72	81.78	100.82	0.81	0.1047	0.0023	4.4439	0.1031	0.3060	0.0046	1.709.3	36.1	1.720.6	19.3	1.720.9	22.8	99%
73	152.05	310.06	0.49	0.0668	0.0014	1.2387	0.0300	0.1331	0.0021	831.5	44.4	818.3	13.6	805.7	12.1	98%
74	250.28	267.18	0.94	0.0643	0.0015	1.1857	0.0300	0.1328	0.0021	753.7	249.1	794.0	13.9	803.9	12.0	98%

续表 2-2
Continued Table 2-2

测点	$w_b/10^{-6}$		Th/U		同位素比值		年齡 Ma		谐和度							
	^{232}Th	^{238}U	$^{207}\text{Pb}/^{206}\text{Pb}$	1σ	$^{207}\text{Pb}/^{235}\text{U}$	1σ	$^{206}\text{Pb}/^{238}\text{U}$	1σ	$^{207}\text{Pb}/^{206}\text{Pb}$	1σ	$^{207}\text{Pb}/^{235}\text{U}$	1σ	$^{206}\text{Pb}/^{238}\text{U}$	1σ		
75	64.89	133.50	0.49	0.0512	0.0020	0.4955	0.0189	0.0706	0.0012	250.1	88.9	408.6	12.8	439.5	7.3	92%
76	174.44	191.47	0.91	0.0665	0.0015	1.1723	0.0278	0.1269	0.0018	821.9	50.9	787.7	13.0	770.0	10.1	97%
77	843.76	294.13	2.87	0.0630	0.0014	1.0478	0.0247	0.1197	0.0016	705.6	48.1	727.8	12.3	728.8	8.9	99%
78	107.01	226.31	0.47	0.0546	0.0016	0.5280	0.0156	0.0700	0.0012	398.2	64.8	430.5	10.4	436.3	7.0	98%
79	130.30	258.34	0.50	0.0530	0.0016	0.4850	0.0144	0.0662	0.0010	327.8	66.7	401.5	9.9	413.1	6.0	97%
80	108.58	140.28	0.77	0.1924	0.0042	12.9098	0.2823	0.4832	0.0060	2762.7	35.0	2673.1	20.7	2541.3	26.3	94%
81	237.09	231.37	1.02	0.0666	0.0017	1.1692	0.0325	0.1262	0.0018	833.3	53.7	786.3	15.2	765.9	10.4	97%
82	99.36	141.57	0.70	0.0551	0.0020	0.5125	0.0179	0.0679	0.0012	416.7	81.5	420.2	12.0	423.8	7.0	99%
83	127.25	176.01	0.72	0.0549	0.0020	0.5314	0.0187	0.0698	0.0011	409.3	81.5	432.7	12.4	434.8	6.8	99%
84	71.05	208.73	0.34	0.0559	0.0018	0.5376	0.0176	0.0697	0.0012	455.6	72.2	436.9	11.6	434.5	7.1	99%
85	342.11	463.57	0.74	0.0671	0.0013	1.2970	0.0270	0.1394	0.0019	842.6	42.6	844.4	11.9	841.5	10.5	99%
86	139.22	152.46	0.91	0.0673	0.0020	1.2302	0.0325	0.1321	0.0019	855.6	59.3	814.4	14.8	800.1	11.0	98%
87	378.00	373.15	1.01	0.0659	0.0018	1.2136	0.0273	0.1334	0.0019	1200.0	58.5	806.9	12.5	807.1	10.8	99%
88	188.70	180.93	1.04	0.0689	0.0019	1.1081	0.0294	0.1166	0.0016	896.0	56.3	757.3	14.2	711.0	9.5	93%
89	127.79	87.77	1.46	0.0539	0.0023	0.5260	0.0246	0.0700	0.0014	368.6	63.9	429.2	16.4	436.4	8.5	98%
90	109.57	151.36	0.72	0.0560	0.0019	0.5385	0.0205	0.0694	0.0013	453.8	74.1	437.5	13.5	432.8	7.6	98%
91	181.86	236.26	0.77	0.0667	0.0015	1.2235	0.0292	0.1325	0.0021	829.3	46.3	811.4	13.3	802.3	11.8	98%
92	325.33	523.51	0.62	0.0560	0.0012	0.5692	0.0148	0.0731	0.0012	453.8	46.3	457.5	9.6	454.7	7.1	99%
93	81.75	135.37	0.6	0.0544	0.0018	0.5226	0.0168	0.0699	0.0011	387.1	75.9	426.9	11.2	435.8	6.5	97%
94	521.34	234.88	2.22	0.0831	0.0015	2.4393	0.0459	0.2116	0.0025	1272.2	35.2	1254.3	13.6	1237.2	13.4	98%
95	223.65	226.08	0.99	0.0662	0.0017	1.2245	0.0282	0.1336	0.0021	813.0	49.1	811.8	12.9	808.6	12.2	99%
96	51.14	98.83	0.52	0.0578	0.0019	0.5749	0.0199	0.0721	0.0013	520.4	69.4	461.2	12.8	449.0	7.6	97%
97	67.92	99.25	0.68	0.0564	0.0022	0.5457	0.0203	0.0703	0.0012	477.8	82.4	442.2	13.3	438.1	7.4	99%
98	95.40	149.01	0.64	0.0547	0.0014	0.5291	0.0148	0.0702	0.0011	466.7	57.4	431.2	9.8	437.6	6.7	98%
99	56.10	368.88	0.15	0.0627	0.0011	0.8528	0.0197	0.0984	0.0018	698.2	40.9	626.2	10.8	605.2	10.5	96%
100	168.36	387.64	0.43	0.0558	0.0013	0.5400	0.0121	0.0702	0.0010	442.6	51.8	438.4	8.0	437.3	6.2	99%
101	197.43	238.98	0.83	0.0645	0.0011	1.1858	0.0262	0.1330	0.0020	766.7	37.0	794.0	12.2	805.0	11.7	98%
102	140.93	177.44	0.79	0.0579	0.0015	0.5606	0.0145	0.0709	0.0011	527.8	59.3	451.9	9.5	441.3	6.5	97%
103	77.62	142.10	0.55	0.0543	0.0015	0.5212	0.0155	0.0697	0.0011	383.4	61.1	425.9	10.4	424.4	6.6	98%
104	41.96	75.03	0.56	0.0556	0.0022	0.5337	0.0214	0.0704	0.0012	435.2	88.9	434.2	14.2	438.3	7.2	99%
105	85.07	163.57	0.52	0.0578	0.0016	0.5801	0.0182	0.0728	0.0013	524.1	61.1	464.5	11.7	453.2	7.8	97%
106	183.04	327.21	0.56	0.0555	0.0012	0.5366	0.0134	0.0699	0.0010	431.5	48.1	436.2	8.8	435.7	5.8	99%
107	68.04	131.68	0.52	0.0558	0.0018	0.5326	0.0161	0.0700	0.0011	455.6	10.7	433.6	7.2	435.9	6.7	99%
108	44.15	81.98	0.54	0.0703	0.0017	1.3429	0.0345	0.1386	0.0020	938.9	50.0	864.5	15.0	836.7	11.5	96%
109	62.77	94.78	0.66	0.0572	0.0018	0.5600	0.0179	0.0714	0.0012	498.2	68.5	451.5	11.6	444.3	7.0	98%
110	47.46	104.18	0.46	0.2163	0.0029	17.2597	0.2798	0.5778	0.0087	2953.4	21.9	2949.4	15.7	2939.6	35.5	99%
111	130.75	184.96	0.71	0.0670	0.0013	1.2844	0.0272	0.1388	0.0021	838.9	40.7	838.8	12.1	838.0	12.1	99%
112	102.88	226.85	0.45	0.0659	0.0014	1.2637	0.0288	0.1385	0.0021	805.6	47.2	829.6	12.9	836.2	12.0	99%
113	85.49	98.94	0.86	0.0670	0.0018	1.2292	0.0330	0.1329	0.0019	836.7	55.6	814.0	15.0	804.5	10.9	98%

多数颗粒内部具有较为明显的振荡环带结构, 锆石的 Th/U 值除 29 号测点(0.034)外总体较高(0.14~2.87), 表明了锆石主要是岩浆成因(Pupin, 1980; Corfu *et al.*, 2003)。经过测试分析, 共计取得 113 个年龄测试数据, 其中不谐和数据 2 个, 其余年龄数据可分为 250 Ma(1 个)、540~400 Ma(63 个)、900~

600 Ma(37 个)、1 800~1 200 Ma(3 个)、3 000~2 400 Ma(7 个), 具有 435.5 Ma 和 798.5 Ma 两个主要的年龄峰值。

3.3 Hf 同位素测试结果

在样品中选取了不同年龄的部分锆石进行了 Hf 同位素的测试分析, 分析结果见表 3。

表 3 隆务河组碎屑岩锆石 Hf 同位素数据

Table 3 Hf isotopic compositions of zircons from the Longwuhe Formation clastic rocks

测点编号	年龄/Ma	$^{176}\text{Yb}/^{177}\text{Hf}$	$^{176}\text{Lu}/^{177}\text{Hf}$	$^{176}\text{Hf}/^{177}\text{Hf}$	$\varepsilon\text{Hf}(t)$	t_{DM}/Ma	$t_{2\text{DM}}/\text{Ma}$	$f_{\text{Lu/Hf}}$
10	797	0.014 419	0.000 622 343	0.281 671 0	-21.71	2 193	3 034	-0.98
21	794	0.018 989	0.000 795 944	0.281 798 2	-17.35	2 029	2 765	-0.98
29	250	0.001 244	0.000 045 999	0.282 146 6	-16.65	1 519	2 315	-1.00
39	539	0.023 138	0.000 898 543	0.282 167 3	-9.84	1 524	2 110	-0.97
48	434	0.041 135	0.001 539 360	0.282 284 4	-8.14	1 385	1 924	-0.95
64	432	0.039 089	0.001 484 619	0.282 268 3	-8.75	1 406	1 960	-0.96
69	2 509	0.014 770	0.000 635 457	0.281 275 6	2.32	2 730	2 865	-0.98
79	413	0.028 691	0.001 076 103	0.282 329 5	-6.86	1 305	1 829	-0.97
93	436	0.024 432	0.000 922 709	0.282 367 5	-4.99	1 247	1 729	-0.97
101	805	0.038 780	0.001 444 381	0.281 945 1	-12.26	1 859	2 460	-0.96
104	438	0.016 660	0.000 629 327	0.282 339 0	-5.85	1 277	1 785	-0.98

测试数据表现出范围较宽的 $^{176}\text{Lu}/^{177}\text{Hf}$ (0.000 045 999~0.001 539 360) 和 $^{176}\text{Hf}/^{177}\text{Hf}$ (0.281 275 6~0.282 367 5) 值, $^{176}\text{Lu}/^{177}\text{Hf}$ 均小于 0.002, 表明锆石中放射性成因的 ^{176}Hf 积累很少。样品的 $f_{\text{Lu/Hf}}$ 在 -1.00~-0.95 之间, 平均值为 -0.97, 低于镁铁质地壳的 $f_{\text{Lu/Hf}}$ (-0.34) 和硅铝质地壳的 $f_{\text{Lu/Hf}}$ (-0.72)(Amelin *et al.*, 1999), 因此二阶段模式年龄更能反

映其源区物质从亏损地幔中被抽取的时间。绝大多数锆石具有负 $\varepsilon\text{Hf}(t)$ 值(-21.71~-4.99), 表明这些碎屑锆石主要来源于地壳物质的再循环, 二阶段模式年龄分布在 3 034~1 729 Ma 之间; 仅有一个样点给出了正 $\varepsilon\text{Hf}(t)$ 值, 对应的二阶段模式年龄为 2 865 Ma(图 6), 意味着该时期存在一定程度的亏损地幔来源, 是物源区地壳生长的一个重要阶段。

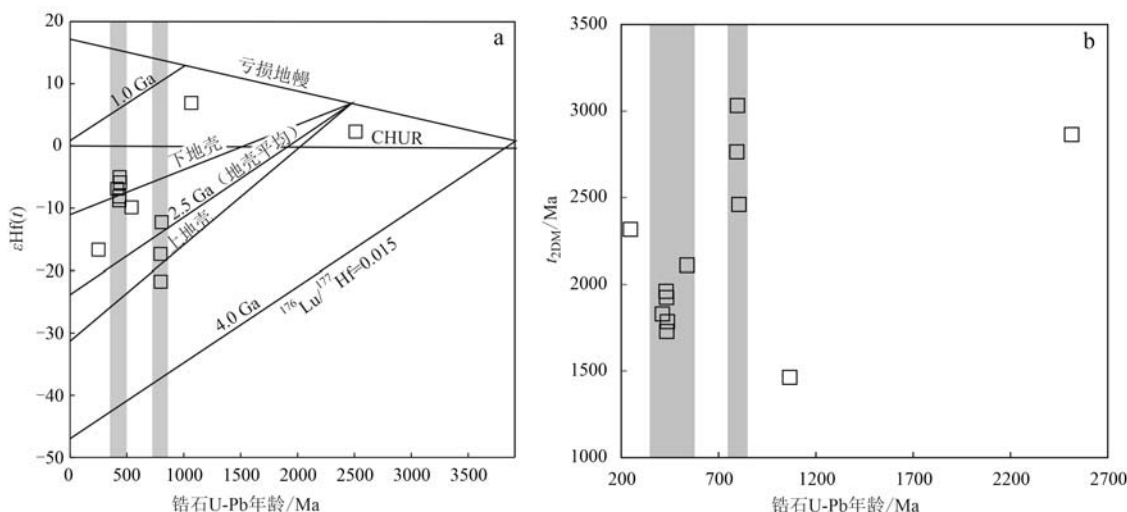


图 6 隆务河组碎屑岩碎屑锆石 $\varepsilon\text{Hf}(t)$ -U-Pb 年龄图(a)和二阶段 Hf 模式年龄-U-Pb 年龄图(b)

Fig. 6 Plots of $\varepsilon\text{Hf}(t)$ -U-Pb age (a) and two-stage Hf model age-U-Pb age (b) for detrital zircons in clastic rocks from Longwuhe Formation

亏损地幔、球粒陨石及平均地壳演化线据 Blichert-Toft *et al.*, 1997; Griffin, 2000

depleted mantle, chondrite and average crustal evolution lines from Blichert-Toft *et al.*, 1997 and Griffin, 2000

4 讨论

4.1 隆务河组源区风化及沉积再循环作用

源区风化、矿物分馏和构造环境等方面的因素共同控制着碎屑沉积岩的化学成分与矿物组成(Bauluz *et al.*, 2000)。碎屑岩的主量和微量元素组成能够为分析物源和构造环境提供有效信息(McLennan, 1993; Zimmerman and Bahlburg, 2003)。化学风化指数通常用来描述岩层的风化程度, CIA 指标是使用最为广泛的指标之一(Rieu *et al.*, 2007; 廖昕等, 2013; 巫锡勇等, 2016), CIA 指标值的增加能够反映随着源岩化学风化程度的增加, 黏土矿物中 Al 元素的富集作用使得 Al_2O_3 含量的增加, 同时硅酸盐类矿物中碱金属、碱土金属元素的风化分解导致 K_2O 和 Na_2O 的含量降低。CIA = 50~65 被看作是轻微风化, CIA = 65~80 代表中等风化, CIA ≥ 85 则指示强烈风化(Fedo *et al.*, 1995)。隆务河组样品的 CIA 值分布于 54.98~57.21 之间, 略高于未经风化上地壳的 CIA 标准值(48; Rudnick and Gao, 2003), 低于 PAAS(70) 和克拉通页岩(77; Condie, 1993) 的 CIA 标准值, 表明隆务河组碎屑岩经历了轻微的风化。与 CIA 指数相似, 斜长石蚀变指数 PIA 通常被用来单独描述斜长石的风化程度,

新鲜岩石的 PIA 指数为 50 (Fedo *et al.*, 1995), 隆务河组碎屑岩样品的 PIA 值为 55.22~59.42, 和上地壳标准值(57; Rudnick and Gao, 2003)接近, 远低于 PAAS 标准值(82; McLennan, 1993), 同样表明了样品经历的风化作用十分轻微。根据质量平衡原理、矿物稳定性热力学计算和长石淋滤实验提出的大陆化学风化趋势 A-CN-K 图解可以分析源岩的风化和钾交代程度(Nesbitt and Young, 1984)。样品投影在长石-钾长石连接线左半部(图 7a), 表明其未经历强烈风化, 样品投影点形成的连线偏离 A-CN 理想风化趋势线, 表明样品经历了一定的钾交代作用, 总体表现为经受了轻微~中等程度的风化作用。ICV 成分变异指数是评价岩石物质成熟度的常用指数(Cox *et al.*, 1995; Potter *et al.*, 2005), 低 ICV 值代表着碎屑沉积岩来自于富含黏土矿物的沉积源区, 其成熟度较高, 往往是被动环境下沉积物的再循环, 而 ICV 值高的碎屑沉积岩则指示了沉积物在构造环境活跃条件下的初次循环(Kamp and Leake, 1985)。隆务河组样品的 ICV 值为 1.53~1.56, 高于 PAAS (0.88; Taylor and McLennan, 1985), 而 CIA 指数低于 PAAS, 表明样品的成熟度较低, 来自于活动构造环境下轻微风化的物源区(图 7b)。

4.2 锯齿年龄谱信息

早期地壳岩石在漫长的地质演化中, 往往经受

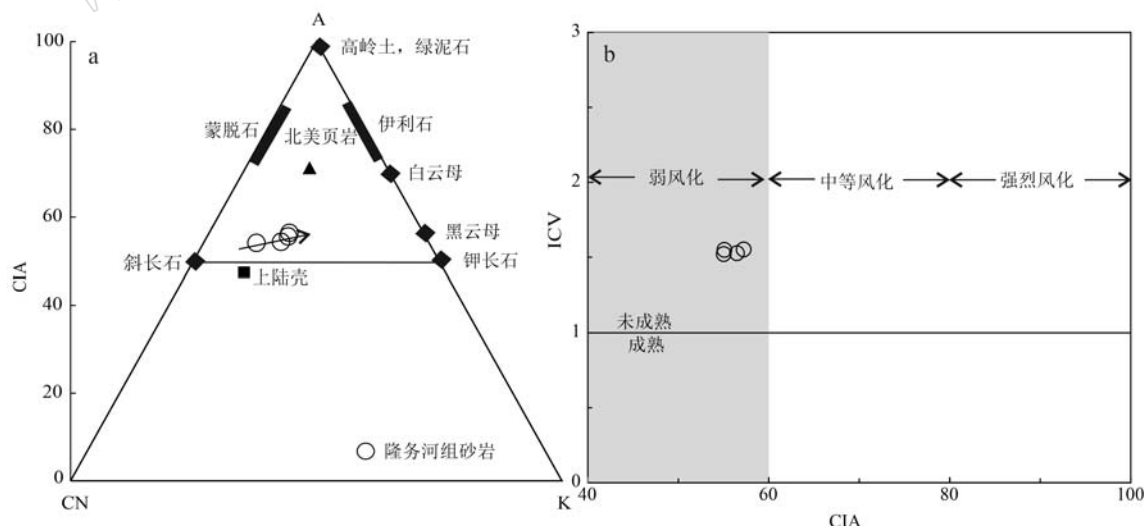


图 7 隆务河组碎屑岩 A-CN-K 图解(a, 据 Fedo *et al.*, 1995) 和 ICV-CIA 图解(b, 据 Nesbitt and Young, 1984; Cox *et al.*, 1995)

Fig. 7 A-CN-K (a, Fedo *et al.*, 1995) and ICV-CIA (b, Nesbitt and Young, 1984; Cox *et al.*, 1995) diagrams for the Longwuhe Formation clastic rocks

了改造和长时间的风化剥蚀, 导致很多古老岩体已不复存在。碎屑岩或变碎屑岩及河流细砂等沉积物作为早期地壳物质的后期混合样品, 能够记录地壳演化过程中出露很少或并未得以保存的岩石信息(第五春荣等, 2012)。沉积岩中的碎屑锆石是极为稳定的副矿物, 封闭性很高, 具有很强的抗风化能力和抗干扰性, 其岩浆锆石年龄是地层形成以后岩浆侵入作用的时间记录, 因此利用碎屑锆石及其岩浆锆石结晶年龄谱系可以追溯蚀源区古老地体所经历的构造-热事件活动历程(Dickinson and Gehrels, 2009), 运用碎屑岩中的碎屑锆石年龄谱数据还可以对地层沉积时代进行有效的约束(Valladares *et al.*, 2004)。通过将碎屑锆石 U-Pb 测年数据与周围出露岩体年龄进行比对, 可以了解源区的多样性和不同期次物源性质的变化特征, 年龄峰值则大致可以确定每一期构造-热事件的年龄范围, 同样也是示踪区域岩浆-变质事件的重要信息(钟玉芳等, 2006)。

在隆务河组样品中, 总共只有 10 颗锆石年龄属于新元古代之前, 1 颗锆石年龄为晚古生代, 均占比较小, 本文主要讨论新元古代及早古生代两个主要的年龄区间。

4.2.1 新元古代年龄信息

样品的碎屑锆石年龄分布于新元古代的共有 37 颗, 占比为 33.3%, 表明新元古代岩石是隆务河组碎屑岩重要的源岩, 年龄分布于 885~605 Ma 之间, 峰值年龄为 798.5 Ma, 可进一步分为 885~836 Ma 和 814~605 Ma 两组。新元古代岩浆活动广泛发育在祁连和柴北缘地区, 大致可分为 2 期(1 000~850 Ma 和 800~730 Ma)(Lu, 2001; Lu *et al.*, 2008; Li *et al.*, 2010; Song *et al.*, 2010; Tung *et al.*, 2012, 2013; Yu *et al.*, 2013; Fu *et al.* 2019), 分别对应于 Rodinia 超大陆的汇聚和裂解事件。孙健等(2018)分析了德令哈市石底泉地区宗务隆构造带内的花岗闪长岩, 认为其具有岛弧或活动大陆边缘花岗岩的属性, 原岩可能为新元古代早期(870.0 ± 4.5 Ma)硅铝地壳或地壳物质熔融的产物。祁连地区也广泛存在新元古代大洋消减的记录, 如 Li 等(2020)通过研究中祁连湟源群中的云母片岩和长英质片麻岩, 认为存在初始洋内俯冲序列(约 1 317~967 Ma)和连续的洋壳-大陆俯冲序列(约 967~896 Ma), Wu 等(2016)证实了祁连地区 1 005~910 Ma 的弧型花岗岩带, Tung 等(2012, 2013)通过对祁连地区新元古

代花岗岩(SHRIMP U-Pb 年龄为 919 ± 10 Ma 和 905 ± 6 Ma)的研究认为, 它们可能形成于岛弧环境, 祁连地区还存在 917 Ma 和 940~930 Ma 的同碰撞花岗岩(郭进京等, 1999; Wan *et al.*, 2000), Yan 等(2015)对化隆群中碎屑锆石的研究同样显示了南祁连 940~780 Ma 的岩浆活动。柴北缘鱼卡-沙柳河高压-超高压变质带内也广泛发育新元古代花岗质片麻岩, 如沙柳河糜棱岩化花岗片麻岩锆石 U-Pb 年龄为 917 ± 21 Ma, 绿梁山一带花岗闪长岩锆石 U-Pb 年龄为 803 ± 7 Ma(陆松年等, 2002), 鱼卡河花岗片麻岩年龄为 855 ± 37 Ma 和 844 ± 15 Ma, 锡铁山全集河钾长花岗片麻岩锆石 U-Pb 年龄为 855 ± 37 Ma(陆松年等, 2006)等, 说明柴北缘晋宁期最重要的巨型花岗岩带形成于侵位于新元古代初期(陆松年等, 2002; 郝国杰等, 2004; 任军虎等, 2011), 样品中 885~836 Ma 的年龄数据应当是这一阶段 Rodinia 聚合事件的反映。柴北缘绿梁山的滩涧山群中存在一套新元古代时期的蛇绿岩组合, 其 Rb-Sr 同位素等时线年龄值为 768 ± 39 Ma, Sm-Nd 同位素等时线年龄值为 780 ± 22 Ma, 全吉群石英梁组底部产出的海底喷溢玄武岩(738 ± 28 Ma)也代表了同时代的裂解作用(李怀坤等, 2003), 南祁连的夏拉诺尔辉长岩中得到 738 ± 11 Ma 的年龄(秦宇, 2018), 表明祁连和柴北缘地区的新元古代-早古生代大洋可能是在 Rodinia 超大陆发生裂解($800 \sim 680$ Ma)的基础上形成的(杨经绥等, 2003; Yang *et al.*, 2006, Wu *et al.*, 2016), 样品中 814~605 Ma 的年龄数据可能代表了这一阶段 Rodinia 超大陆的裂解事件。

4.2.2 早古生代年龄信息

样品中早古生代年龄的碎屑锆石数量最大, 共有 63 颗锆石年龄分布在 540~400 Ma 之间, 峰值年龄为 435.5 Ma, 占比约为 56.8%, 表明早古生代岩石是隆务河组群碎屑岩最重要的源岩。约自 800 Ma 以来, 随着 Rodinia 超大陆的持续裂解, 初始裂谷向洋盆不断发展, 沿柴北缘造山带出露有大量形成于俯冲环境下的岛弧火山岩, 它们主要形成于 535~460 Ma(史仁灯等, 2003; Shi *et al.*, 2006; 王惠初, 2006; 高晓峰等, 2010; Fu *et al.*, 2019, 2021; 张建新等, 2021), 同时, 柴北缘造山带内陆壳岩石的超高压变质时代($458 \sim 420$ Ma)(Song *et al.*, 2004, 2006; Chen *et al.*, 2009; Zhang *et al.*, 2009; Li *et al.*, 2019)及同碰撞花岗岩的成岩时代($450 \sim 420$ Ma)(吴才来等, 2004, 2008; Fu *et al.*, 2021)共同

表明, 柴北缘洋可能在 460~450 Ma 就已经彻底关闭, 并发生陆-陆碰撞形成柴北缘加里东造山带, 在志留纪期间, 造山带遭受强烈隆升和剥蚀, 于泥盆纪早期进入造山后伸展作用阶段(朱小辉等, 2015; 秦宇, 2018)。祁连造山带为一条加里东期增生造山带, 介于柴达木和阿拉善地块之间, 一般认为祁连洋于早寒武世开始俯冲最终经陆-陆碰撞造就了祁连加里东碰撞造山带(夏林圻等, 1998; Song et al., 2013), 南祁连地区自西向东断续发育有党河南山-拉脊山早古生代蛇绿岩带(肖序常等, 1978; 邱家骥等, 1998), 形成年龄为 530~480 Ma(Fu et al., 2018; 宋述光等, 2019); 西段 SSZ 型蛇绿岩形成于 539~522 Ma(Yan et al., 2019) 和 441 Ma(黄增保等, 2016), 东段基性-超基性岩体侵位于 450~441 Ma(张照伟等, 2015), 并发育奥陶纪洋内弧火山岩(Song et al., 2017), 表明南祁连洋整体的北向俯冲可能始于中奥陶世末期, 中奥陶世末-早志留世岩浆岩(462~430 Ma)反映了南祁连洋消亡和南祁连造山带形成过程中的构造-岩浆活动(张照伟等, 2015; 黄增保等, 2016; Wu et al., 2016, 2021; 秦宇, 2018)。约 430~402 Ma 俯冲板片断离, 造成地壳熔融, 北祁连地区因地壳明显加厚, 发生下地壳拆沉(刘秀婷, 2019), 与此同时, 南祁连地区也进入了碰撞后的伸展阶段(430~375 Ma)(Wu et al., 2016, 2021)。上述研究显示, 柴北缘早古生代花岗质岩浆作用主要集中于 475~460 Ma 和 450~440 Ma, 分别对应于洋壳俯冲(岛弧或活动大陆边缘)和陆-陆碰撞阶段(同碰撞环境)(朱小辉等, 2015), 而南祁连地区的岩浆活动则主要发育于 462~430 Ma, 样品中碎屑锆石的年龄可进一步分为 539~490 Ma(2 颗)、462~432 Ma(54 颗)、429~408 Ma(7 颗)这 3 个年龄区间。相比于柴北缘, 缺少了 475~463 Ma 的年龄数据, 而与南祁连的岩浆记录十分相似。3 个年龄区间应当代表了南祁连地区在早古生代初期持续的裂解、中奥陶世末—早志留世的俯冲碰撞和之后的造山后伸展作用。

综上所述, 隆务河组碎屑岩中早古生代锆石可能主要由北侧的南祁连提供。而彭渊等(2018)通过对附近宗务隆群的分析, 认为相邻宗务隆群(C-P₂)物源区是柴北缘。可能的情况是, 早古生代造山后, 相对于柴北缘, 南祁连并未隆升, 而南侧的柴

北缘在宗务隆裂谷开始发育时是沉积物的主要来源, 随着宗务隆裂谷的闭合, 在早中三叠世, 西段的宗务隆山已经隆起, 北侧南祁连的巴龙贡噶尔组随之成为区内主要的物源区。

4.3 沉积时代与构造环境

碎屑锆石年龄中最年轻的锆石年龄经常被用来约束地层的最大沉积时代(沉积下限)(Fedo et al., 1996; Dickinson and Gehrels, 2009; Tucker et al., 2013)。样品中最年轻的碎屑锆石年龄为 249.6 Ma, 但该年龄的数据仅有一个, 除此之外较年轻的年龄记录为 429~408 Ma(7 颗), 表明隆务河组沉积时代在志留纪之后。在 1:5 万的区域地质调查工作中, 本区隆务河组灰岩中发现瓣鳃类化石 *Chlamys* sp., 页岩中发现孢粉化石 *Calamospora impeaa Playtora*、*Micrhystridum Setasessitante Jansonius*、*Punetatisporites* sp.、*Reticulatisporites pudens Balme*、*Veryhachium trispinosum* 等(青海省地质调查院, 2006)^①, 均为早中三叠世的常见分子, 综合基础地质资料及锆石年龄分析, 认为其沉积时代应为早三叠世—中三叠世。

不同构造环境下形成的碎屑岩, 其地球化学成分有所区别, 因而分析碎屑岩的地球化学成分是研究古构造环境的有效手段之一(Bhatia, 1983; Taylor and McLennan, 1985; Bhatia and Crook, 1986; McLennan, 1993)。样品与不同构造背景下碎屑岩的地球化学特征(表 4)显示, 样品的地球化学指标基本处于活动大陆边缘-大陆岛弧环境的范围内。

在 $TiO_2-(Fe_2O_3^T+MgO)$ 和 K_2O/Na_2O-SiO_2 判别图解中(图 8a、8b), 样品投影在活动大陆边缘-大陆岛弧区域, 在 $Sc-La-Th$ 图解中样品落入大陆岛弧、活动大陆边缘与被动大陆边缘的区域(图 8c), 在 $Th-Sc-Zr/10$ 图解中样品均落在大陆岛弧区域(图 8d)。

岩石的地球化学指标往往具有多解性(Bhatia and Crook, 1986; Rudnick and Gao, 2003), 其地球化学特征也可能代表了物源区的构造环境, 因而, 判别沉积岩形成的构造环境还需要结合区域地质演化进行分析。前人研究柴北缘加里东期造山运动时认为 446.3 ± 3.9 Ma 和 420~410 Ma 两个重要事件段代表了柴达木地块与祁连地块碰撞的时代和深俯冲折返的时代(吴才来等, 2007)。结合宗务隆构造带

^① 青海省地质调查院. 2006. 青海省德令哈市宗务隆山地区六幅 1:5 万区域报告.

表4 隆务河组碎屑沉积岩与不同构造环境下碎屑沉积岩微量元素特征值对比表

Table 4 Comparison of the geochemical characteristics of the Longwuhe Formation clastic rocks and clastic rocks from various tectonic settings

	大洋岛弧	大陆岛弧	活动大陆边缘	被动大陆边缘	样品值域范围	样品平均值
$w(\text{Fe}_2\text{O}_3^T + \text{MgO})/\%$	11.73	6.79	4.63	2.89	5.87~6.76	8.59
$w(\text{TiO}_2)/\%$	1.06	0.64	0.46	0.49	0.48~0.60	0.52
$w(\text{K}_2\text{O})/w(\text{Na}_2\text{O})$	0.39	0.61	0.99	1.6	0.80~1.66	1.35
$w(\text{Al}_2\text{O}_3)/w(\text{SiO}_2)$	0.29	0.2	0.18	0.1	0.14~0.18	0.15
$w(\text{La})/10^{-6}$	8	27	37	39	27.97~48.72	36.26
$w(\text{Ce})/10^{-6}$	19	59	78	85	48.97~85.07	64.34
$w(\Sigma \text{REE})/10^{-6}$	58	146	186	210	127.23~206.12	159.28
$w(\text{LREE})/w(\text{HREE})$	3.8	7.7	9.1	8.5	7.96~10.84	8.98
δEu	1.04	0.79	0.6	0.56	0.37~1.52	1.06
$w(\text{La})/w(\text{Y})$	0.48	1.02	1.33	1.31	1.39~2.09	1.63
$w(\text{Rb})/w(\text{Sr})$	0.05	0.65	0.89	1.19	0.20~0.34	0.28
$w(\text{Th})/w(\text{Sc})$	0.15	0.85	2.59	3.06	1.16~1.43	1.29
$w(\text{Zr})/w(\text{Th})$	48	21.5	9.5	19.1	11.63~14.79	13.07

表中大洋岛弧、大陆岛弧、活动大陆边缘和被动大陆边缘值据 Bhatia (1983)、Bhatia 和 Crook (1986)。

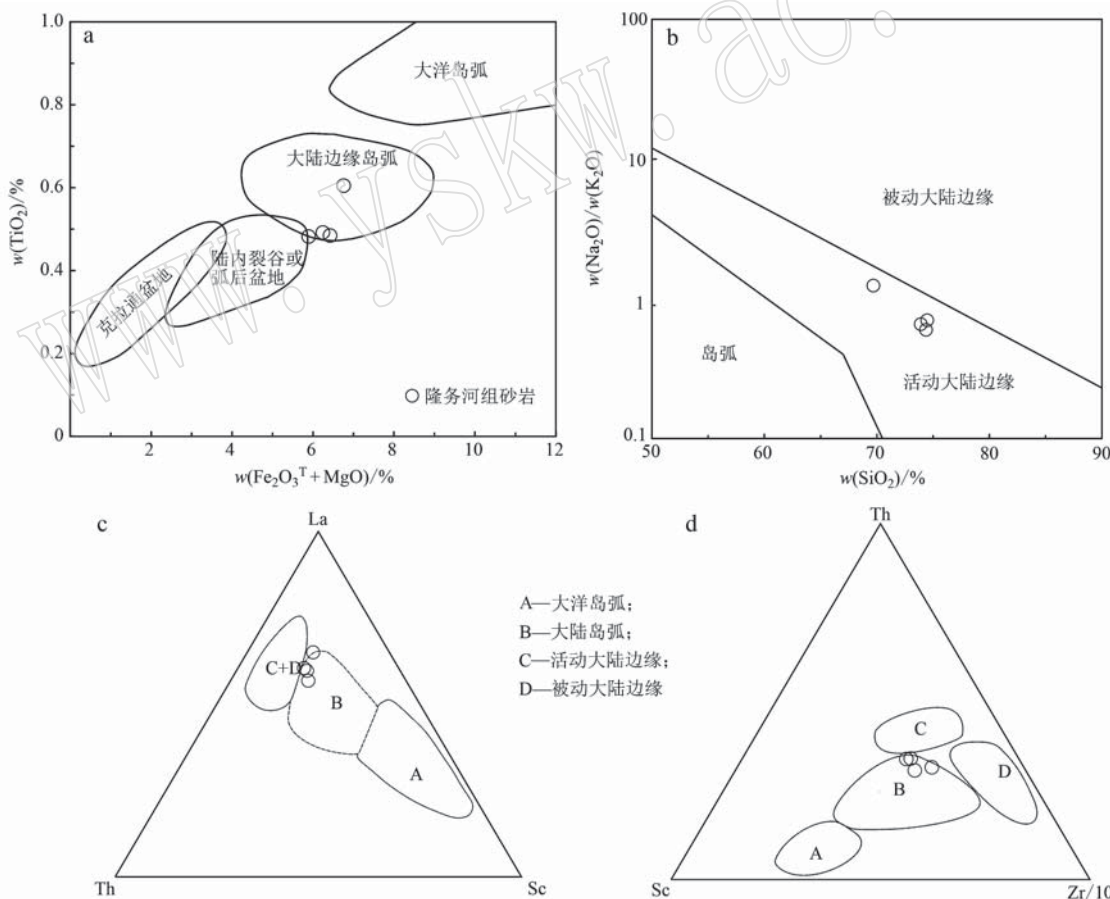


图8 隆务河组碎屑岩的 $\text{TiO}_2 - (\text{Fe}_2\text{O}_3^T + \text{MgO})$ (a, 据 Bhatia, 1983)、 $\text{K}_2\text{O}/\text{Na}_2\text{O}-\text{SiO}_2$ (b, 据 Roser and Korsch, 1986)、

Fig. 8 $(\text{Fe}_2\text{O}_3 + \text{MgO})-\text{TiO}_2$ (a, Bhatia, 1983), $\text{K}_2\text{O}/\text{Na}_2\text{O}-\text{SiO}_2$ (b, Roser and Korsch, 1986), $\text{Sc}-\text{La}-\text{Th}$ (c, Bhatia and Crook, 1986) and $\text{Th}-\text{Sc}-\text{Zr}/10$ (d, Bhatia and Crook, 1986) tectonic setting discrimination diagrams for the Longwuhe Formation clastic rocks

周缘泥盆系的发育(张雪亭等, 2010)和宗务隆带东南苦海-赛什塘带拉龙洼泥盆纪辉绿岩墙群的出现(393.5 ± 3.0 Ma, Ar/Ar 年龄)(孙延贵等, 2004)以及察汗诺角闪辉长岩 416 ± 5 Ma(彭渊, 2015)的发现, 意味着区域整体进入了加里东期造山运动结束后的伸展作用阶段。宗务隆构造带可能在此背景下发生了拉张裂陷, 随后于晚石炭世(318 Ma, Rb/Sr 年龄)出现宗务隆洋盆(王毅智等, 2001), 洋壳向南的俯冲活动发生于晚二叠世—中三叠世期间并形成乌兰北东以中酸性火山岩为代表的岛弧地体(郭安林等, 2009; 王苏里等, 2016; 彭渊等, 2016; Wu et al., 2019), 宗务隆洋壳的俯冲大约持续了 40 Ma, 在中晚三叠世发生闭合(王苏里等, 2016)。上述研究主要集中在宗务隆构造带东段乌兰—青海南山的区域, 在构造带的西段, 庄玉军等(2020)在欧龙布鲁克地块西北缘发现早石炭世辉长岩脉(锆石 U-Pb 年龄 357 ± 4 Ma), 认为早石炭世柴北缘仍处于后造山伸展扩张的构造演化阶段, 德令哈西巴罗根郭勒的基性岩墙(U-Pb 年龄, 289 ± 1 Ma)表现出为板内碱性玄武岩的特征(陈敏等, 2020), 这表明在宗务隆构造带东段天峻南山有限洋盆发育时, 西段地区仍为板内环境, 样品给出的碎屑锆石的年龄在 $408 \sim 249$ Ma 之间完全空白, 也暗示西段隆务河组的沉积物中未能包含宗务隆构造带俯冲闭合和碰撞的岩浆记录。而在采样点以东的生格地区, 土尔根大坂组的碎屑锆石年龄则拥有 $404 \sim 206$ Ma 的完整记录(赵文涛等, 2020), 这与宗务隆构造带东段晚古生代—中生代强烈的岩浆活动也能够很好地对应。从沉积特征来看, 构造带西段的隆务河组表现出磨拉石建造的特征, 而东段具有复理石建造的特征, 也显示了东西段构造环境的差异。因而, 宗务隆带的东段具有俯冲碰撞的有限洋盆, 而西段可能是未发育洋盆的裂谷, 两者之间的转换地带可能在生格到罗根郭勒之间。在东段的俯冲碰撞作用发生时, 西段地区则表现为早期的裂谷盆地在挤压隆升背景下的构造反转, 从而缺乏相应的岩浆事件, 可能由挤压推覆形成的褶皱冲断带引起了地壳的挠曲变形, 在宗务隆山前沉积了隆务河组的碎屑岩。

5 结论

(1) 宗务隆构造带罗根郭勒地区隆务河组碎屑岩的岩石学和地球化学特征表明, 其物源区古风化

程度轻微, 不具备“沉积再循环”特征, 源岩主要为长英质岩石。南祁连新元古代花岗质片麻岩和早古生代大陆弧型花岗岩可能为隆务河组碎屑岩的主要物源。

(2) 宗务隆构造带西段的隆务河组碎屑岩可能形成于早中三叠世褶皱冲断引起的挠曲型盆地中。

(3) 宗务隆构造带东西段的构造演化具有不同的历程, 东段发育有限洋盆, 而西段并未出现, 转换地带可能在生格到罗根郭勒之间。

致谢 感谢编辑部的辛勤工作和审稿专家的宝贵意见, 感谢在野外地质考察期间青海省地质调查院李玉龙和赵志逸两位同志提供的帮助, 在此一并致谢!

References

- Amelin Y, Lee D C, Halliday A N, et al. 1999. Nature of the Earth's earliest crust from Hafnium Isotopes in Single detrital Zircons [J]. Nature, 399: 1 497~1 503.
- Bauluz B, Mayayo M J, Fernandez-Nieto C, et al. 2000. Geochemistry of Precambrian and Paleozoic siliciclastic rocks from the Iberian Range-NE Spain: Implication for source-area weathering, sorting, provenance, and tectonic setting[J]. Chemical Geology, 168: 135~150.
- Bhatia M R. 1983. Plate tectonics and geochemical composition of sandstones[J]. Journal of Geology, 91: 611~627.
- Bhatia M R and Crook K. 1986. Trace element characteristics of graywackes and tectonic setting discrimination of sedimentary basins [J]. Contributions to Mineralogy & Petrology, 92(2): 181~193.
- Blichert-Toft J, Chauvel C and Albarè De F. 1997. Separation of Hf and Lu for high-precision isotope analysis of rock samples by magnetic sector-multiple collector Icp-Ms[J]. Contributions to Mineralogy & Petrology, 127(3): 248~260.
- Cawood P A and Nemchin A A. 2000. Provenance record of a rift basin: U/Pb ages of detrital zircons from the Perth Basin, Western Australia [J]. Sedimentary Geology, 134: 209~234.
- Chen Min, Xue ChunJi, Xue Wanwen, et al. 2020. Discovery and geological significance of Xuji diorite in Zongwulong tectonic belt on the northern margin of Qaidam Basin[J]. Acta Petrologica et Mineralogica, 39(5): 44~60 (in Chinese with English abstract).
- Chen Nengsong, Gong Songlin, Sun Min, et al. 2009. Precambrian evolution of the Quanji Block, northeastern margin of Tibet: Insights from zircon U-Pb and Lu-Hf isotope compositions[J]. Journal of

- Asian Earth Sciences, 35(3~4): 367~376.
- Condie K C. 1993. Chemical composition and evolution of the upper continental crust: Contrasting results from surface samples and shales [J]. Chemical Geology, 104(1~4): 1~37.
- Corfu F, Hanchar J M, Hoskin P W O, et al. 2003. Atlas of zircon textures [J]. Reviews in Mineralogy and Geochemistry, 53(1): 469~500.
- Cox R, Lowe D R and Cullers R L. 1995. The influence of sediment recycling and basement composition on evolution of mudrock chemistry in the southwestern United States[J]. Geochimica et Cosmochimica Acta, 59: 2 919~2 940.
- Dickinson W R and Gehrels G E. 2009. Use of U-Pb ages of detrital zircons to infer maximum depositional ages of strata: A test against a Colorado Plateau Mesozoic database[J]. Earth & Planetary Science Letters, 288(1~2): 115~125.
- Diwu Chunrong, Sun Yong and Wang Qian. 2012. The crustal growth and evolution of North China Craton: Revealed by Hf isotopes in detrital zircons from modern rivers[J]. Acta Petrologica Sinica, 28(11): 3 520~3 530(in Chinese with English abstract).
- Fedo C M, Eriksson K A and Krogstad E J. 1996. Geochemistry of shales from the Archean (~3.0 Ga) Buhwa Greenstone Belt, Zimbabwe: Implications for provenance and source-area weathering[J]. Geochimica et Cosmochimica Acta, 60(10): 1 751~1 763.
- Fedo C M, Nesbitt H W and Young G M. 1995. Unraveling the effects of potassium metasomatism in sedimentary rocks and paleosoils, with implication for paleoweathering conditions and provenance[J]. Geology, 23: 921~924.
- Fu Changlei, Yan Zhen, Aitchison Jonathan C, et al. 2021. Short-lived intra-oceanic arc-trench system in the North Qaidam belt (NW China) reveals complex evolution of the Proto-Tethyan Ocean[J]. GSA Bulletin, <https://doi.org/10.1130/B36127.1>
- Fu Changlei, Yan Zhen, Guo Xianqing, et al. 2019. Assembly and dispersal history of continental blocks within the Altun-Qilian-North Qaidam mountain belt, NW China[J]. International Geology Review, 61(4): 424~447.
- Fu Changlei, Yan Zhen, Wang Zongqi, et al. 2018. Lajishankou ophiolite complex: Implications for Paleozoic multiple accretionary and collisional events in the South Qilian Belt[J]. Tectonics, 37(5): 1 321~1 346.
- Fu Changlei, Yan Zhen, Xiao Wenjiao, et al. 2021. Identification and geological significance of the Early Paleozoic Tianjunnanshan remnant ocean basin in the Zongwulong belt, NE Tibetan Plateau[J]. Acta Petrologica Sinica, 37(8): 2 401~2 418(in Chinese with English abstract).
- Gao Xiaofeng, Li Wenyuan, Ye Meifang, et al. 2010. Geochemistry of amphibolites in Hualong Group of eastern Middle Qilian massif and its tectonic significance [J]. Journal of Rock Mineralogy, 29 (5): 507~515(in Chinese with English abstract).
- Griffin W L. 2000. The hf isotope composition of cratonic mantle: LAM-MC-ICPMS analysis of zircon megacrysts in kimberlites [J]. Geochimica et Cosmochimica Acta, 64(1): 133~147.
- Guo Anlin, Zhang Guowei, Qiang Juan, et al. 2009. Indosinian Zongwulong orogenic belt on the northeastern margin of the Qinghai-Tibet plateau[J]. Acta Petrologica Sinica, 25 (1): 1~12 (in Chinese with English abstract).
- Guo Jingjing, Zhang Guowei, Lu Songnian, et al. 1999. Analysis for sedimentary-tectonic setting of the Huangyuan Group in the estern Mid-Qilian Massif, Qilian Orogenic Belt[J]. Journal of Northwest University: Natural Science Edition, 29 (4): 343~347(in Chinese with English abstract).
- Hallsworth C R, Morton A C, Clague-Long J, et al. 2000. Carboniferous sand provenance in the Pennine Basin, UK: Constraints from heavy mineral and detrital zircon age data[J]. Sedimentary Geology, 137: 147~185.
- Hao Guojie, Lu Songnian, Wang Huichu, et al. 2004. The Pre-Devonian tectonic framework in the northern margin of Qaidam Basin and geological evolution of Olongbuluck Palaeo-block [J]. Earth Science Frontiers, 11(3): 115~122(in Chinese with English abstract).
- He Xiaoyuan, Yang Xingke, Wang Yong, et al. 2021. Geochemical and zircon U-Pb chronology of the volcanic rocks from the Balonggonggaer Formation in Tuergendaban, southern Qilian Mountain [J]. Acta Geologica Sinica, 95 (3): 750~764 (in Chinese with English abstract).
- Huang Zengbao, Zheng Jianping, Li Baohua, et al. 2016. Age and geochemistry of the Early Paleozoic back-arc type ophiolite in Dadaoerji Area, South Qilian, China[J]. Geotectonica et Metallogenica, 40 (4): 826~838(in Chinese with English abstract).
- Ji Bo, Li Xiangmin, Huang Botao, et al. 2021. Detrital zircon U-Pb geochronology of the Neoproterozoic Guaizhangshan Group in Danghenanshan area of the South Qilian Mountains and its geological significance[J]. Acta Geologica Sinica, 95 (3): 765~778 (in Chinese with English abstract).
- Ji Bo, Yu Jiyuan, Li Xiangmin, et al. 2018. The disintegration of Balonggongge'er Formation and the definition of lithostratigraphic unit in Danghenanshan area of South Qilian Mountain: Evidence from petrology and chronology[J]. Geological Bulletin of China, 37 (4): 621~633(in Chinese with English abstract).

- Joo Y J, Lee Y and Bai Z Q. 2005. Provenance of the Qingshuijian Formation (Late Carboniferous), NE China: Implications for tectonic processes in the northern margin of the North China block [J]. *Sedimentary Geology*, 177(12): 97~114.
- Kamp P C and Leake B E. 1985. Petrography and geochemistry of feldspathic and mafic sediments of the northeastern Pacific margin [J]. *Transactions of the Royal Society of Edinburgh: Earth Sciences*, 76(4): 411~499.
- Li Dalei, Sun Dongliang, Zhao Zhenying, et al. 2018. Geological characteristics and age of Balonggungar Formation in Xiawu area, Delingha City, Qinghai [J]. *Geological Bulletin of China*, 37(4): 634~641 (in Chinese with English abstract).
- Li Huaikun, Lu Songnian, Wang Huichu, et al. 2003. Quanji Group—the geological record of the Rodinia supercontinent break-up in the Early Neoproterozoic preserved in the northern Qaidam margin, Qinghai, Northwest China [J]. *Geological Survey and Research*, 26(1): 27~37, 60 (in Chinese with English abstract).
- Li Meng, Wang Chao, Li Rongshe, et al. 2019. Identifying late Neoproterozoic-early Paleozoic sediments in the South Qilian Belt, China: A peri-Gondwana connection in the northern Tibetan Plateau [J/OL]. *Gondwana Research*, 76: 174~184. doi: 10.1016/j.gr.2019.06.010.
- Li Xianhua, Li Wuxian, Li Qiuli, et al. 2010. Petrogenesis and tectonic significance of the similar to 850 Ma Gangbian alkaline complex in South China: Evidence from in situ zircon U-Pb dating, Hf-O isotopes and whole-rock geochemistry [J]. *Lithos*, 114(1~2): 1~15.
- Li Ping'an and Nie Shuren. 1982. Structural characteristics of Zongwulong aulacogen [J]. *Geology of Qinghai*, 2: 65~76 (in Chinese).
- Liao Fanxi, Zhang Lu, Chen Nengsong, et al. 2014. Geochronology and geochemistry of meta-mafic dykes in the Quanji Massif, NW China: Paleoproterozoic evolution of the Tarim Craton and implications for the assembly of the Columbia supercontinent [J]. *Precambrian Research*, 249: 33~56.
- Liao Xin, Wu Xiyong and Zhu Baolong. 2013. Chemical weathering characteristics of cambrian black shale in northern Guangxi, China [J]. *Journal of Central South University (Science and Technology)*, 44(12): 4 980~4 987 (in Chinese with English abstract).
- Liu Kui, Li Zongxing, Shi Xiaobin, et al. 2020. Late Hercynian-Indosinian denudation and uplift history in the eastern Qaidam Basin: Constraints from multiple thermometric indicators and sedimentary evidences [J]. *Chinese J. Geophys*, 63(4): 1 403~1 421 (in Chinese with English abstract).
- Liu Xiuting. 2019. Spatial-temporal Distribution and Tectonic Implications of Granitoids from Qilian Block [D]. Chinese Academy of Sciences (Qinghai Institute of Salt Lakes), 1~85 (in Chinese with English abstract).
- Liu Yongsheng, Gao Shan, Hu Zhaochu, et al. 2010. Continental and oceanic crust recycling-induced melt-peridotite interactions in the Trans-North China Orogen: U-Pb dating, Hf isotopes and trace elements in zircons from mantle xenoliths [J]. *Journal of Petrology*, 51: 537~571.
- Lu Zenglong, Zhang Jianxin, Mao Xiaohong, et al. 2017. Paleoproterozoic basic granulites in the eastern part of oulongbrooke block on the northern margin of Qaidam: Petrology, zircon U-Pb chronology and Lu-Hf isotopic evidence [J]. *Acta Petrologica Sinica*, 33(12): 3 815~3 828 (in Chinese with English abstract).
- Lu Songnian. 2001. Major Precambrian events in northwestern China [J]. *Gondwana Research*, 4(4): 692~692.
- Lu Songnian, Ding Haifeng, Li Huaikun, et al. 2006. Study on Major Geological Problems of Precambrian in China—Major Geological Event Group of Precambrian in Western China and Its Global Tectonic Significance [M]. Beijing: Geological Publishing House, 175~193 (in Chinese).
- Lu Songnian, Li Huaikun, Zhang Chuanlin, et al. 2008. Geological and geochronological evidence for the precambrian evolution of the Tarim craton and surrounding continental fragments [J]. *Precambrian Research*, 160(1~2): 94~107.
- Lu Songnian, Wang Huichu, Li Huaikun, et al. 2002. Redefinition of the “Dakendaban Group” on the northern margin of the Qaidam basin [J]. *Geological Bulletin of China*, 21(1): 19~23 (in Chinese with English abstract).
- Ma Shuai, Chen Shiyue, Sun Jiaopeng, et al. 2016. The early Paleozoic lithofacie-palaeogeography of Olongbluk micro-massif on the northern margin of Qaidam Basin [J]. *Geology in China*, 43(6): 2 011~2 021 (in Chinese with English abstract).
- McLennan S M. 1993. Weathering and global denudation [J]. *The Journal of Geology*, 101: 295~303.
- McLennan S M, Hemming S R, Taylor S R, et al. 1995. Early Proterozoic crustal evolution: Geochemical and Nd-Pb isotopic evidence from metasedimentary rocks, southwestern North America [J]. *Geochimica et Cosmochimica Acta*, 59(6): 1 153~1 177.
- McLennan S M, Simonetti A and Goldstein S L. 2000. Nd and Pb isotopic evidence for provenance and post-depositional alteration of the Paleoproterozoic Huronian Supergroup, Canada [J]. *Precambrian Research*, 102(3~4): 263~278.
- Nesbitt H W and Young C M. 1982. Early Proterozoic climates and plate

- motions inferred from major element chemistry of lutites [J]. *Nature*, 199: 715~717.
- Nesbitt H W and Young G M. 1984. Prediction of some weathering trends of plutonic and volcanic rocks based on thermodynamic and kinetic considerations [J]. *Geochimica et Cosmochimica Acta*, 48 (7): 1 523~1 534.
- Niu Guangzhi, Huang Gang, Deng Changsheng, et al. 2016. LA-ICP-MS zircon U-Pb age of metamorphic volcanic rocks of Balonggonggar Formation in Qilian, Qinghai Province and its geological significance [J]. *Geological Bulletin of China*, 35 (9): 1 441~1 447 (in Chinese with English abstract).
- Pan Jian, Li Guiyi and Li Guangtie. 2019. Re-division of Balonggonggaer Formation in Qinghai Province and its geological significance [J]. *Global Geology*, 38 (4): 900~909 (in Chinese with English abstract).
- Peng Yuan. 2015. The Late Hercynian-Indosinian Structural Characteristics of the Zongwulong Tectonic Belt in North Qaidam Basin [D]. Beijing: Chinese Academy of Geological Sciences, 1~164 (in Chinese with English abstract).
- Peng Yuan, Ma Yinsheng, Liu Chenglin, et al. 2016. Geological characteristics and tectonic significance of the Indosinian granodiorites from the Zongwulong tectonic belt in North Qaidam [J]. *Earth Science Frontiers*, 23(2): 206~221 (in Chinese with English abstract).
- Peng Yuan, Zhang Yongsheng, Sun Jiaopeng, et al. 2018. Provenance and tectonic setting of the Zhongwunongshan Group from the Zhongwunongshan structural belt and its adjacent areas in North Qaidam, China: Evidence from geochemistry and detrital zircon geochronology [J]. *Geotectonica et Metallogenesis*, (1): 126~149 (in Chinese with English abstract).
- Peng Zhijun, Wu Pandeng, Liu Songbai, et al. 2016. An analysis of sediments characteristics of Early-Middle Triassic Longwuhe Formation from Guomaying area in Guinan County, Qinghai Province [J]. *Geological Bulletin of China*, 35(9): 1 506~1 511 (in Chinese with English abstract).
- Potter P E, Maynard J B and Depetris P J. 2005. Mud and Mudstones [M]. Berlin: Springer-Verlag Heidelberg Publication, 157~166.
- Pupin J P. 1980. Zircon and granite petrology [J]. *Contributions to Mineralogy and Petrology*, 73(3): 207~220.
- Qin Yu. 2018. Neoproterozoic to Early Paleozoic Tectonic Evolution in the South Qilian Orogen [D]. Xi'an: Northwest University, 39~115 (in Chinese with English abstract).
- Qiu Jiaxiang, Zeng Guangce, Zhu Yunhai, et al. 1998. Characteristics and latitudinal comparative research on the early Palaeozoic volcanic rocks of rifted orogenic belt and small ocean basin ophiolite suit from Northern Qinling Mountains and Southern Qilian Mountains [J]. *Geological Journal of China Universities*, (4): 34~46 (in Chinese with English abstract).
- Ren Junhu, Zhang Kun, Liu Yiqun, et al. 2011. Geochemical characteristics and zircon dating of blasto-gabbrro from the South Jinshukou area, Easten Kunlun [J]. *Journal of Northwest University (Natural Science Edition)*, (1): 100~106 (in Chinese with English abstract).
- Rieu R, Allen P A, Plotze M, et al. 2007. Compositional and mineralogical variations in a neoproterozoic glacially influenced succession, mirbat area, south oman: Implications for paleoweathering conditions [J]. *Precambrian Research*, 154(3~4): 248~265.
- Roser B P, Coombs D S and Korsch R J. 2002. Whole-rock geochemical variation and evolution of the arc-derived Murikku Terrane [J]. *New Zealand Geological Magazine*, 139(6): 665~685.
- Roser B P and Korsch R J. 1986. Determination of tectonic setting of sandstone-mudstone suites using SiO₂ content and K₂O/Na₂O ratio [J]. *The Journal of Geology*, 94(5): 635~650.
- Roser B P and Krosch R J. 1988. Provenance signatures of sandstone-mudstone suites determined using discriminant function analysis of major-element data [J]. *Chemical Geology*, 67: 119~139.
- Rudnick R L and Gao Shan. 2003. The composition of the continental crust [J]. *Treatise Geochem.*, 3: 1~64.
- Shi Rendeng, Yang Jingsui and Wu Cailai. 2003. The discovery of adakitic dacite in Early Palaeozoic island arc volcanicrocks on the northern margin of Qaidam Basin and its geological significance [J]. *Acta Petrologica et Mineralogica*, 22 (3): 229~236 (in Chinese with English abstract).
- Shi Rendeng, Yang Jingsui, Wu Cailai, et al. 2006. Island arc volcanic rocks in the north Qaidam UHP belt, northern Tibet plateau: Evidence for ocean-continent subduction preceding continent-continent subduction [J]. *Journal of Asian Earth Sciences*, 28(2~3): 151~159.
- Song Shuguang, Niu Yaoling, Su Li, et al. 2013. Tectonics of the North Qilian orogen, NW China [J]. *Gondwana Research*, 23(4): 1 378~1 401.
- Song Shuguang, Su Li, Li Xianhua, et al. 2010. Tracing the 850-Ma continental flood basalts from a piece of subducted continental crust in the North Qaidam UHMP belt, NW China [J]. *Precambrian Research*, 183(4): 805~816.
- Song Shuguang, Wu Zhenzhu, Yang Liming, et al. 2019. Ophiolite belts and evolution of the Proto-Tethys Ocean in the Qilian Orogen

- [J/OL]. *Acta Petrologica Sinica*, 35(10): 2 948~2 970 (in Chinese with English abstract). doi: 10.18654/1000-0569/2019.10.02
- Song Shuguang, Yang Liming, Zhang Yuqi, et al. 2017. Qi-Qin accretionary belt in Central China Orogen: Accretion by trench jam of oceanic plateau and formation of intra-oceanic arc in the Early Paleozoic Qin-Qi-Kun Ocean[J]. *Science Bulletin*, 62(15): 1 035~1 038.
- Song Shuguang, Zhang Lifei and Niu Yaoling. 2004. Ultra-deep origin of garnet peridotite from the North Qaidam ultrahigh-pressure belt, Northern Tibetan Plateau, NW China[J]. *American Mineralogist*, 89(8~9): 1 330~1 336.
- Song Shuguang, Zhang Lifei, Niu Yaoling, et al. 2006. Evolution from oceanic subduction to continental collision: A case study from the northern Tibetan Plateau based on geochemical and geochronological data[J]. *Journal of Petrology*, 47(3): 435~455.
- Sun Jian, Yang Zhangzhang, Zhao Zhenying, et al. 2018. LA-ICP-MS zircon U-Pb ages and geological significance of granodiorite from Zongwulong tectonic belt in Delingha, Qinghai Province [J]. *Geological Bulletin of China*, 37(4): 604~612 (in Chinese with English abstract).
- Sun Jiaopeng, Chen Shiyue, Peng Yuan, et al. 2015. Determination of Early Cambrian zircon SHRIMP U-Pb datings in Zongwulong tectonic belt, Northern margin of Qaidam Basin, and its geological significance[J]. *Geological Review*, 61(4): 743~751 (in Chinese with English abstract).
- Sun Jiaopeng, Yin Chengming, Chen Shiyue, et al. 2016. An analysis of Late Carboniferous sedimentary tectonic setting and provenance of North Qaidam area: Evidence from Well Shiqian 1[J]. *Geological Bulletin of China*, 35(2/3): 302~310 (in Chinese with English abstract).
- Sun S S and McDonough W F. 1989. Chemical and isotopic systematics of oceanic basalts: Implications for mantle composition and processes [A]. Geological Society, London, Special Publications[C]. 313~345.
- Sun Yangui, Zhang Guowei, Guo Anlin, et al. 2004. Qinling-Kunlun triple junction and isotope chronological evidence of its tectonic process[J]. *Geology in China*, 31(4): 372~378 (in Chinese with English abstract).
- Taylor S R and McLennan S M. 1985. The Continental Crust: Its Composition and Evolution[M]. Oxford: Blackwell Publication, 1~312.
- Tucker R T, Roberts E M, Hu Yi, et al. 2013. Detrital zircon age constraints for the Winton Formation, Queensland: Contextualizing Australia's Late Cretaceous dinosaur faunas [J]. *Gondwana Research*, 24(2): 767~779.
- Tung Kuoan, Yang Houngyi, Liu Dunyi, et al. 2012. The amphibolite-facies metamorphosed mafic rocks from the Maxianshan area, Qilian block, NW China: A record of early Neoproterozoic arc magmatism [J]. *Journal of Asian Earth Sciences*, 46(46): 177~189.
- Tung Kuoan, Yang Houngyi, Liu Dunyi, et al. 2013. The Neoproterozoic granitoids from the Qilian block, NW China: Evidence for a link between the Qilian and South China blocks [J]. *Precambrian Research*, 235: 163~189.
- Valladares C S, Machado N, Heilbron M, et al. 2004. Ages of detrital zircon from siliciclastic successions south of the so francisco craton, brazil: Implications for the evolution of Proterozoic basins[J]. *Gondwana Research*, 7(4): 913~921.
- Wan Yusheng, Yang Jingsui, Xu Zhiqin, et al. 2000. Geochemical characteristics of the Maxianshan Complex and Xinglongshan Group in the eastern segment of the Qilian Orogenic Belt[J]. *Journal of the Geological Society of China*, 43(1): 52~68.
- Wang Huichu. 2006. Early Paleozoic Collisional Orogeny and Magmatism on Northern Margin of the Qaidam Basin[D]. Beijing: China University of Geosciences, 1~159 (in Chinese with English abstract).
- Wang Lu, Johnston S T and Chen Nengsong. 2019. New insights into the Precambrian tectonic evolution and continental affinity of the Qilian block: Evidence from geochronology and geochemistry of metasupracrustal rocks in the North Wulan terrane[J]. *Geological Society of America Bulletin*, 131: 1 723~1 743.
- Wang Lu, Wang Heng, He Chuan, et al. 2016. Mesoproterozoic continental breakup in NW China: Evidence from gray gneisses from the North Wulan terrane[J]. *Precambrian Research*, 281: 521~536.
- Wang Suli and Zhou Lifu. 2016. LA-ICP-MS zircon U-Pb dating, geochemistry and tectonic implication of the bojite in the Zongwulong Mountain[J]. *Journal of Northwest University (Natural Science Edition)*, 46(5): 716~724 (in Chinese with English abstract).
- Wang Yizhi, Bai Yongshan and Lu Hailian. 2001. Geological characteristics of Tianjunnanshan ophiolite in Qinghai and its forming environment[J]. *Qinghai Geology*, 21(1): 29~35 (in Chinese).
- Wu Cailai, Gao Yuanhong, Wu Suoping, et al. 2007. Zircon SHRIMP U-Pb dating of granites from the Da Qaidam area in the north margin of Qaidam basin, NW China[J]. *Acta Petrologica Sinica*, 23(8): 1 861~1 875 (in Chinese with English abstract).
- Wu Cailai, Gao Yuanhong, Wu Suoping, et al. 2008. SHRIMP U-Pb zircon dating and geochemical characteristics of granites in the western part of northern Qaidam Basin[J]. *Chinese Science: Geosciences*, 38(8): 930~949 (in Chinese with English abstract).

- Wu Cailai, Wu Di, Mattinson C, et al. 2019. Petrogenesis of granitoids in the Wulan area: magmatic activity and tectonic evolution in the north Qaidam, NW China[J]. *Gondwana Research*, 147~171.
- Wu Cailai, Yang Jingsui, Xu Zhiqin, et al. 2004. Granitic Magmatism on the Early Paleozoic UHP Belt of Northern Qaidam, NW China [J]. *Acta Geologica Sinaca*, 78(5): 658~674 (in Chinese with English abstract).
- Wu Chen, Yin An, Zuza Andrew V, et al. 2016. Pre-Cenozoic geologic history of the central and northern Tibetan Plateau and the role of Wilson cycles in constructing the Tethyan orogenic system[J/OL]. *Lithosphere*, 8(3): 254~292. <https://doi.org/10.1130/1494.1>
- Wu Chen, Zuza Andrew V, Yin An, et al. 2021. Punctuated orogeny during the assembly of Asia: Tectonostratigraphic evolution of the North China Craton and the Qilian Shan from the Paleoproterozoic to Early Paleozoic[J/OL]. *Tectonics*, 40(4): <https://doi.org/10.1029/2020TC006503>
- Wu Xiyong, Ling Sixiang, Ren Yong, et al. 2016. Elemental migration characteristics and chemical weathering degree of black shale in northeast Chongqing, China[J]. *Earth Science*, 41(2): 218~233 (in Chinese with English abstract).
- Xia linqi, Xia Zuchun and Xu Xueyi. 1998. Early Palaeozoic mid-ocean ridge-ocean island and back-arc basin volcanism in the North Qilian Mountains[J]. *Acta Geologica Sinica*, (4): 301~312 (in Chinese with English abstract).
- Xiao Xuchang, Chen Guoming and Zhu Zhizhi. 1978. A preliminary study on the tectonics of ancient ophiolites in the Qilian Mountain Northwest China[J]. *Acta Geologica Sinica*, (4): 31~88 (in Chinese with English abstract).
- Yan Zhen, Aitchison J, Fu Changlei, et al. 2015. Hualong Complex, South Qilian terrane: U-Pb and Lu-Hf constraints on Neo-proterozoic micro-continental fragments accreted to the northern proto-Tethyan margin[J]. *Precambrian Research*, (266): 65~85.
- Yan Zhen, Fu Changlei, Aitchison J C, et al. 2019. Early Cambrian Mu-li arc-ophiolite complex: A relic of the Proto-Tethys oceanic lithosphere in the Qilian Orogen, NW China[J]. *International Journal of Earth Sciences*, 108: 1147~1164.
- Yan Zhen, Fu Changlei, Aitchison J C, et al. 2020. Silurian sedimentation in the South Qilian Belt: Arc-continent collision-related deposition in the NE Tibet Plateau? [J]. *Acta Geologica Sinica*, 94(4) : 901~913.
- Yang Jingsui, Wu Cailai, Zhang Jianxin, et al. 2006. Protolith of eclogites in the north Qaidam and Altun UHP terrane, NW China: Earlier oceanic crust? [J]. *Journal of Asian Earth Sciences*, 28(2~3) : 185~204.
- Yang Jingsui, Xu Zhiqin, Ma Changqian, et al. 2010. Compound orogeny and scientific problems concerning the Central Orogenic Belt of China [J]. *Geology in China*, 37 (1): 1~11 (in Chinese with English abstract).
- Yang jingsui, Zhang Jianxin, Meng Fancong, et al. 2003. Ultrahigh pressure eclogites of the North Qaidam and Altun mountains, NW China and their protoliths[J]. *Earth Science Frontiers*, 10(3): 291~314 (in Chinese with English abstract).
- Yu Shengyao, Zhang Jianxin, del Real Pablo Garcia, et al. 2013. The Grenvillian orogeny in the Altun-Qilian-North Qaidam mountain belts of northern Tibet Plateau: Constraints from geochemical and zircon U-Pb age and Hf isotopic study of magmatic rocks[J]. *Journal of Asian Earth Sciences*, 73(8): 372~395.
- Yu Shengyao, Zhang Jianxin and Li Sanzhong. 2017. Paleoproterozoic granulite-facies metamorphism and anatexis in the Oulongbuluke Block, NW China: Respond to assembly of the Columbia supercontinent[J]. *Precambrian Research*, 291: 42~62.
- Zhang Haifan, Wang Xunlian, Wang Xun, et al. 2016. U-Pb zircon ages of tuffbeds from the Hongzaoshan Formation of the Quanji Group in the north margin of the Qaidam Basin, NW China, and their geological significances[J]. *Earth Science Frontiers*, 23(6): 202~21 (in Chinese with English abstract).
- Zhang Jianxin, Lu Zenglong, Mao Xiaohong, et al. 2021. Revisiting the Precambrian micro-continental blocks within the Early Paleozoic orogenic system of the northeastern Qinghai-Tibet Plateau: Insight into the origin of Proto-Tethyan Ocean[J]. *Acta Petrologica Sinica*, 37 (1): 74~94 (in Chinese with English abstract).
- Zhang R Y, Liou J G, Iizuka Yoshiyuki, et al. 2009. First record of K-cymrite in North Qaidam UHP eclogite, Western China[J]. *American Mineralogist*, 94(2~3): 222~228.
- Zhang Xueting, Yang Shengde and Yang Zhanjun. 2010. Introduction to Regional Geology of Qinghai Province: 1:1 Million Geological Map of Qinghai Province[M]. Beijing: Geological Publishing House, 1~84 (in Chinese).
- Zhang Zhaowei, Wang Yalei, Qian Bing, et al. 2015. Mineralization characteristics and metallogenetic regularity of mafic-ultramafic intrusions in Hualong area, Qinghai Province[J]. *Geology in China*, 42 (3): 724~736 (in Chinese with English abstract).
- Zhao Wentao, Liu Shaofeng and Chen Min. 2020. Detrital zircon geochronology and its geological significance from turgendaban formation in Shengge area of Zongwulong structural belt[J]. *China Mining Magazine*, 29(S1): 279 ~283 (in Chinese with English abstract).

- Zhong Yufang, Ma Changqian and She Zhenbing. 2006. Review of zircon geochemical characteristics and geological application[J]. Geological Science and Technology Information, 1: 27~34, 40 (in Chinese).
- Zimmerman U and Bahlburg H. 2003. Provenance analysis and tectonic setting of the Ordovician clastic deposits in the southern Puna Basin, NW Argentina[J]. Sedimentology, 50: 1 079~1 104.
- Zhu Xiaohui, Chen Danling, Wang Chao, et al. 2015. The Initiation, Development and Termination of the Neoproterozoic-Early Paleozoic Ocean in the North Margin of Qaidam Basin[J]. Acta Geologica Sinica, 89(2): 234~251 (in Chinese with English abstract).
- Zhuang Yujun, Gu Pingyang, Gao Yongwei, et al. 2020. Petrogenesis of Middle Permian gabbro in Saishiteng Mountain of the northern Qaidam Basin and its constraint to the time of Zongwulong Ocean subduction[J]. Acta Petrologica et Mineralogica, 39(6): 78~734 (in Chinese with English abstract).

附中文参考文献

- 陈敏,薛春纪,薛万文,等. 2020. 柴北缘宗务隆构造带蓄集地区闪长岩的发现及其地质意义[J]. 岩石矿物学杂志, 39(5): 44~60.
- 第五春荣,孙勇,王倩. 2012. 华北克拉通地壳生长和演化:来自现代河流碎屑锆石Hf同位素组成的启示[J]. 岩石学报, 28(11): 3 520~3 530.
- 付长奎,闫臻,肖文交,等. 2021. 青藏高原东北缘宗务隆构造带天峻南山早古生代残余洋盆的识别和地质意义[J]. 岩石学报, 37(8): 2 401~2 418.
- 高晓峰,李文渊,叶美芳,等. 2010. 中祁连东段化隆群中斜长角闪岩地球化学特征及构造意义[J]. 岩石矿物学杂志, 29(5): 507~515.
- 郭安林,张国伟,强娟,等. 2009. 青藏高原东北缘印支期宗务隆造山带[J]. 岩石学报, 25(1): 1~12.
- 郭进京,张国伟,陆松年,等. 1999. 中祁连地块东段元古宙基底涅源群沉积构造环境[J]. 西北大学学报(自然科学版), 29(4): 343~347.
- 郝国杰,陆松年,王惠初,等. 2004. 柴达木盆地北缘前泥盆纪构造格架及欧龙布鲁克古陆块地质演化[J]. 地学前缘, 11(3): 115~122.
- 贺小元,杨兴科,王永,等. 2021. 南祁连土尔根达坂巴龙贡噶尔组火山岩地球化学及锆石U-Pb年代学研究[J]. 地质学报, 95(3): 750~764.
- 黄增保,郑建平,李葆华,等. 2016. 南祁连大道尔吉早古生代弧后盆地型蛇绿岩的年代学、地球化学特征及意义[J]. 大地构造与成矿学, 40(4): 826~838.
- 计波,李向民,黄博涛,等. 2021. 南祁连党河南山地区新元古代拐杖山岩群碎屑锆石U-Pb年代学及其地质意义[J]. 地质学报, 95(3): 765~778.
- 计波,余吉远,李向民,等. 2018. 南祁连党河南山地区巴龙贡噶尔组的解体与岩石地层单位厘定——来自岩石学与年代学的证据[J]. 地质通报, 37(4): 621~633.
- 李大磊,孙东亮,赵振英,等. 2018. 青海德令哈市夏吾一带巴龙贡噶尔组地质特征及时代[J]. 地质通报, 37(4): 634~641.
- 李怀坤,陆松年,王惠初,等. 2003. 青海柴北缘新元古代超大陆裂解的地质记录——全吉群[J]. 地质调查与研究, 26(1): 27~37, 60.
- 李平安,聂树人. 1982. 宗务隆裂陷槽的构造特征[J]. 青海地质, 2: 65~76.
- 廖听,巫锡勇,朱宝龙. 2013. 桂北地区寒武系黑色页岩化学风化特征[J]. 中南大学学报(自然科学版), (12): 4 980~4 987.
- 刘奎,李宗星,施小斌,等. 2020. 柴达木盆地东部晚海西-印支期剥蚀量与隆升历史——多种古温标与沉积学证据的制约[J]. 地球物理学报, 63(4): 1 403~1 421.
- 刘秀婷. 2019. 祁连地块花岗岩类时空分布及其地质意义[D]. 中国科学院大学(中国科学院青海盐湖研究所), 1~85.
- 路增龙,张建新,毛小红,等. 2017. 柴北缘欧龙布鲁克地块东段古元古代基性麻粒岩:岩石学、锆石U-Pb年代学和Lu-Hf同位素证据[J]. 岩石学报, 33(12): 3 815~3 828.
- 陆松年,丁海峰,李怀坤,等. 2006. 中国前寒武纪重大地质问题研究——中国西部前寒武纪重大地质事件群及其全球构造意义[M]. 北京: 地质出版社, 175~193.
- 陆松年,王惠初,李怀坤,等. 2002. 柴达木盆地北缘“达肯大坂群”的再厘定[J]. 地质通报, 21(1): 19~23.
- 马帅,陈世悦,孙娇鹏,等. 2016. 柴达木盆地北缘欧龙布鲁克微地块早古生代岩相古地理[J]. 中国地质, 43(6): 2 011~2 021.
- 牛广智,黄岗,邓昌生,等. 2016. 青海南祁连巴龙贡噶尔组变火山岩LA-ICP-MS锆石U-Pb年龄及其他地质意义[J]. 地质通报, 35(9): 1 441~1 447.
- 潘建,李贵义,李广铁. 2019. 青海省巴龙贡噶尔组的重新划分及地质意义[J]. 世界地质, 38(4): 900~909.
- 彭渊. 2015. 柴北缘宗务隆构造带海西晚期—印支期构造特征研究[D]. 中国地质科学院, 1~164.
- 彭渊,马寅生,刘成林,等. 2016. 柴北缘宗务隆构造带印支期花岗闪长岩地质特征及其构造意义[J]. 地学前缘, 23(2): 206~221.
- 彭渊,张永生,孙娇鹏,等. 2018. 柴北缘北部中吾农山构造带及

- 邻区中吾农山群物源和构造环境: 来自地球化学与锆石年代学的证据[J]. 大地构造与成矿学, (1): 126~149.
- 彭志军, 吴攀登, 刘松柏, 等. 2016. 青海省贵南县过马营一带早中三叠世隆务河组沉积特征[J]. 地质通报, 35(9): 1 506~1 511.
- 秦宇. 2018. 南祁连造山带新元古代—早古生代构造演化[D]. 西安: 西北大学, 39~115.
- 邱家骥, 曾广策, 朱云海, 等. 1998. 北秦岭-南祁连早古生代裂谷造山带火山岩与小洋盆蛇绿岩套特征及纬向对比[J]. 高校地质学报, (4): 34~46.
- 任军虎, 张琨, 柳益群, 等. 2011. 东昆仑金水口南变余辉长岩地球化学及锆石定年[J]. 西北大学学报(自然科学版), (1): 100~106.
- 史仁灯, 杨经绥, 吴才来. 2003. 柴北缘早古生代岛弧火山岩中埃达克质英安岩的发现及其地质意义[J]. 岩石矿物学杂志, 22(3): 229~236.
- 宋述光, 吴珍珠, 杨立明, 等. 2019. 祁连山蛇绿岩带和原特提斯洋演化[J]. 岩石学报, 35(10): 2 948~2 970.
- 孙健, 杨张张, 赵振英, 等. 2018. 青海石底泉地区宗务隆构造带花岗闪长岩 LA-ICP-MS 锆石 U-Pb 年龄及其地质意义[J]. 地质通报, 37(4): 604~612.
- 孙娇鹏, 陈世悦, 彭渊, 等. 2015. 柴达木盆地北缘宗务隆构造带早古生代锆石 SHRIMP 年龄的测定及其地质意义[J]. 地质论评, 61(4): 743~751.
- 孙娇鹏, 尹成明, 陈世悦, 等. 2016. 柴达木盆地北缘晚石炭世构造环境及物源——以石浅 1 井为例[J]. 地质通报, 35(2~3): 302~311.
- 孙延贵, 张国伟, 郭安林, 等. 2004. 秦—昆三向联结构造及其构造过程的同位素年代学证据[J]. 中国地质, 31(4): 372~378.
- 王惠初. 2006. 柴达木盆地北缘早古生代碰撞造山带及岩浆作用[D]. 北京: 中国地质大学(北京), 1~159.
- 王苏里, 周立发. 2016. 宗务隆山角闪辉长岩 LA-ICP-MS 锆石 U-Pb 定年、地球化学特征及其地质意义[J]. 西北大学学报(自然科学版), 46(5): 716~724.
- 王毅智, 拜永山, 陆海莲. 2001. 青海天峻南山蛇绿岩的地质特征及其形成环境[J]. 青海地质, (1): 29~35.
- 巫锡勇, 凌斯祥, 任勇, 等. 2016. 渝东北黑色页岩元素迁移特征及化学风化程度[J]. 地球科学, 41(2): 218~233.
- 吴才来, 鄢源红, 吴锁平, 等. 2007. 柴达木盆地北缘大柴旦地区古生代花岗岩锆石 SHRIMP 定年[J]. 岩石学报, (8): 1 861~1 875.
- 吴才来, 鄢源红, 吴锁平, 等. 2008. 柴北缘西段花岗岩锆石 SHRIMP U-Pb 定年及其岩石地球化学特征[J]. 中国科学: 地球科学, 38(8): 930~949.
- 吴才来, 杨经绥, 许志琴, 等. 2004. 柴达木盆地北缘古生代超高压带中花岗质岩浆作用[J]. 地质学报, 78(5): 658~674.
- 夏林圻, 夏祖春, 徐学义. 1998. 北祁连山早古生代洋脊-洋岛和弧后盆地火山作用[J]. 地质学报, (4): 301~312.
- 肖序常, 陈国铭, 朱志直. 1978. 祁连山古蛇绿岩带的地质构造意义[J]. 地质学报, (4): 31~88.
- 杨经绥, 张建新, 孟繁聪, 等. 2003. 中国西部柴北缘-阿尔金的超高压变质榴辉岩及其原岩性质探讨[J]. 地学前缘, 10(3): 291~314.
- 杨经绥, 许志琴, 马昌前, 等. 2010. 复合造山作用和中国中央造山带的科学问题[J]. 中国地质, 37(1): 1~11.
- 张海军, 王训练, 王勋, 等. 2016. 柴达木盆地北缘全吉群红藻山组凝灰岩锆石 U-Pb 年龄及其地质意义[J/OL]. 地学前缘, 23(6): 202~218. DOI: 10.13745/j.esf.2016.06.014.
- 张建新, 路增龙, 毛小红, 等. 2021. 青藏高原东北缘早古生代造山系中前寒武纪微陆块的再认识——兼谈原特提斯洋的起源[J]. 岩石学报, 37(1): 74~94.
- 张雪亭, 杨生德, 杨站军. 2010. 青海省区域地质概论——1:100 万青海省地质图说明书[M]. 北京: 地质出版社, 1~84.
- 张照伟, 王亚磊, 钱兵, 等. 2015. 青海省化隆地区镁铁-超镁铁质侵入岩含矿特点与成矿规律[J]. 中国地质, 42(3): 724~736.
- 赵文涛, 刘少峰, 陈敏. 2020. 宗务隆构造带生格地区土尔根大坂组碎屑锆石年代学及其地质意义[J]. 中国矿业, 29(S2): 234~240.
- 钟玉芳, 马昌前, 余振兵. 2006. 锆石地球化学特征及地质应用研究综述[J]. 地质科技情报, 1: 27~34, 40.
- 朱小辉, 陈丹玲, 王超, 等. 2015. 柴达木盆地北缘新元古代-早古生代大洋的形成、发展和消亡[J]. 地质学报, 89(2): 234~251.
- 庄玉军, 姜平阳, 高永伟, 等. 2020. 柴北缘赛什腾中二叠世辉长岩成因及其对宗务隆洋盆俯冲时限的制约[J]. 岩石矿物学杂志, 39(6): 78~734.